2012

Expanding the usable workspace of a haptic device by placing it on a moving base

Isaac Garlington
Iowa State University

Expanding the usable workspace of a haptic device by placing it on a moving base

by

Isaac Joel Garlington

A thesis submitted to the graduate faculty

in partial fulfillment of the requirements for the degree of

MASTER OF SCIENCE

Major: Mechanical Engineering

Program of Study Committee:
Judy M. Vance, Co-Major Professor
Greg R. Luecke, Co-Major Professor
Derrick K. Rollins

Iowa State University

Ames, Iowa

2012

Table Of Contents

LIST OF FIGURES

LIST OF TABLES

ABSTRACT

The goal of this research is to expand the reachable workspace of a haptic device when used in a projection screen virtual environment. The proposed method includes supplementing the haptic device with a redundant degree of freedom to provide motion of the base. The key research challenge is to develop controls for the mobile base that will keep the haptic end-effector in the usable haptic workspace at all times. An experimental set up consisting of an Omni haptic device and a XY motorized table was used in the development of the control algorithms. Tests were conducted which demonstrate that the force felt by the user when touching a virtual wall remains constant even when the mobile base is moving to re-center the haptic device in the usable haptic workspace.

Chapter 1 Introduction

An area of research in virtual reality investigates methods for increasing the sensory feedback for the user so the experience seems more realistic. Haptics is provided as a powerful tool that provides force and tactile feedback for a virtual environment. Haptics is an enhancement to virtual environments that allows users to "touch" and feel the simulated objects that they interact with [1]. Haptic devices are commonly used for training medical students to perform minimally-invasive surgeries and teaching human anatomy [2]. The need for haptic devices to accomplish assembly tasks similar to work cell environments has raised interest in increasing the reachable haptic workspace. This discussion has led to the creation of large-scale haptics. Large-scale haptics could play a major role in how the automotive and aerospace industries understand the ergonomics of their virtual assembly processes. Determining the most effective way to increase the reachable haptic workspace for Large-Scale Haptics is of fundamental significance to the field of Virtual Reality because the sensory feedback is affected depending on how the reachable workspace of the haptic manipulators is increased.

Large-scale haptics is a relatively unknown area because there are many researchers have different methods as to how to increase the reachable workspace of the haptic device, but there is not a method that addresses problems such as producing a high force output while maintaining transparency, and . There are currently four main methods for increasing the reachable workspace of a haptic device which include using a wearable haptic interface, utilizing tensed cable robots such as the Spidar (Space Interface Device for Artificial Reality),

installing a redundant axis to the haptic device, and utilizing a mobile haptic interface [3]. The understanding is small and there are a lot of questions left for using mobile robots to increase the reachable workspace of a haptic device. Specifically, the overall contribution of this work is to implement a haptic arm force-feedback device within an increased reachable workspace by way of using a redundant degree of freedom within a stationary, stereoscopic display.

Chapter 2 Background

2.1 Virtual Reality

Virtual Reality is an artificial environment composed of interactive computer simulations that sense the participant's positions and actions, providing synthetic feedback to one or more senses, giving the feeling of being immersed or being present in the reality [4]. For the user, virtual reality provides stimuli for visual, aural, haptic (touch), vestibular, olfaction, and gestation to increase the immersiveness. One of the strengths of Virtual Reality is that it is a beneficial tool for collaboration because it has the ability to put multiple users in the same virtual space regardless of the physical distance that may separate the users. The field of Virtual Reality has existed for over half-a-century and as more and more technological advancements made it to market, this technology is used in electronic industry for video games, manufacturing industry for product design, and in training simulators for complex jobs like being a commercial pilot.

2.2 History

In 1956, the first concept of Virtual Reality was created by Morton Heilig. Helig was a cinematographer and inventor who created the Sensorama. The Sensorama is a multimodal experience in which the user sits in front of a display equipped with sensory stimulators such as sound, wind, smell, and vibration. They were composed of scenarios such as driving a motorcycle through an environment [5].

In 1963, Ivan Sutherland demonstrated what is known as the Sketchpad. This is the first use of computer-generated visual imagery that was displayed on a cathode ray tube. Two years later, he envisioned an immersive, computer-based, synthetic world that included visual, aural, and haptic feedback to the user. In 1968, Sutherland demonstrated a system that visualized a stick representation of a three dimensional cyclo-hexane molecule. It used a head mounted tracking system to detect the user's position. Myron Krueger also developed virtual reality using a different point of view. He provided a 2nd person view of the user so that the users would be watching themselves in the virtual world. A lot of this technology was fascinating, but in order for the field to advance, there needed to be technological advancements in graphics engines, head-mounted displays, etc., which was later accomplished by the University of North Carolina at Chapel Hill [6].

In 1977, an additional tool was created for position feedback from the user's hand to the computer simulation for use in virtual reality. The Sayre glove was created at the University of Illinois at Chicago that was outfitted to sense the bend of the participant's fingers [7]. The CAVE visual display was also created at the University of Illinois at Chicago in 1992. The CAVE is a projection-based virtual reality system configured with three or more surfaces projected with stereoscopic, head tracked, computer graphics [8].

2.3 Visual Display Methods

Three primary methods of visual display are used for virtual reality. Those three different displays are stationary displays, head-mounted displays, and hand-mounted displays.

Stationary displays do not move as the user changes their position relative to the real world. A common example of a stationary display is a CAVE (Cave Automatic Virtual Environment) created by the Electronic Visualization Laboratory at the University of Illinois at Chicago. The information that is graphically rendered is dependent on the user's position for a stereoscopic visual representation. One such application at Iowa State University includes working with John Deere utilizing a Deere tractor buck mounted in a CAVE configuration, with a detailed model of a particular Iowa farm in 1999 [9].

Head-Mounted Displays (HMD) keep the visual display in front of the user's eyes at all times. Therefore only one display screen for each eye is needed. In industry, Head-Mounted Displays are commonly referred to as HMDs. The first patent for Head-Mounted Display was in 1974 by Richard Mostrom with the original application being intended for pilots [10]. Hand-Mounted Displays are visual displays that are held in the user's hand. A major difference between Hand-Mounted Displays and HMDs is that the Hand-Mounted Displays allow the user has the ability to look around the real world as well as look at the virtual world.

2.4 Navigation

Craig and Sherman [11] discuss the tools for navigation in the virtual world and illustrate each method. There are two parts to navigation in a virtual environment called Wayfinding and Travel. Wayfinding is the Virtual Reality system using the world information to determine the position, speed, and the direction of travel of the user. The second part, Travel, is how the user moves within that virtual world. There are 9 common travel paradigms that are used for virtual environments.

The Physical Locomotion travel method in virtual reality is the ability for the user to move his body to change the position and point of view within the virtual environment. It is commonly used in most Virtual Reality Applications in combination with another form of travel.

The Ride-Along travel method offers little choice for the user. The path is already predetermined. With this form of locomotion, users typically are allowed to look around and change their point of view while they are on that predetermined path. This method is similar to riding as the passenger in a vehicle where the driver is driving in a direction given by a Global Positioning System, and the passenger has the opportunity to "enjoy the scenery." The Tow-Rope travel method is very similar to the Ride-along method. The difference is that the participant has the opportunity to move from the centerline of the path for a small distance. This is similar to a snowmobile pulling a snow sled. The snowmobile may have a specific path, but the snow sled attached by a tow-rope is allowed to drift from the exact path the snowmobile took.

Using the Fly-Through travel method gives the user almost complete control of how they move (Forward, Backward, Left, Right, Downward, and Upward). Very close to this method is the Walk-Through Method where the user may move in any direction, but is constrained to following the virtual terrain as they would be if they were at standing height above it. In the Pilot-Through travel method, users control the virtual movements using controls that closely resemble the vehicle that they are riding in. An example would be a flight simulator that has the same cockpit setup as the plane the pilot would be flying in real life.

Move-The-World locomotion lets the user "grab" the world and bring it nearer or re-position it in general by moving and orientating their hand in a particular manner. Scale-the-

World allows the user to make the virtual world "shrink," followed by the user making a small movement to move, and shortly afterward the virtual world returns to its original size. Both of these previous two methods involve manipulation of the virtual environment in order to traverse throughout it.

The following two methods of travel are the least natural forms of travel for the user. In the travel method called Put-Me-Here, the user specifies the exact position that they would like to be at in the virtual world, and the simulation would take the user there instantly. It's very similar to the idea of teleportation seen in many science fiction movies today, with the exception that it takes the user's virtual representation and put that virtual representation somewhere else in space. Orbital-viewing is considered the least natural form of travel in comparison to Put-Me-Here. It appears that the object rotates around the user when the user rotates their head. If an object was in front of the user, the user looks upward, the object would rotate so that the user would be looking at the bottom of the object.

2.5 Other Virtual Reality Technologies

There are several other terms associated with virtual reality technology; however, they are not restricted to only in discussions with virtual reality.

Augmented reality is an altered view or altered perception of the real world, and uses the user's physical location for this altered perception. The availability of augmented reality applications has accelerated for smart phones in recent years. A major strength for augmented reality is that it has the capability to add information to the user's sensory input.

Telepresence virtually places one user in another location that they may not be physically present. Many of us use telepresence everyday without realizing it. A common instance of Telepresence that society uses consistently is a telephone or video conference. Smart phone applications such as Skype, FaceTime, or Tango all give users the capability to include the visual stimuli of seeing the user as well as hearing the voice with aural stimuli.

2.6 Haptics

Virtual Prototyping is the process of evaluating a new design on a computer without the need of possessing a physical prototype. As a result of this technology, products have a smaller cycle time (from conception to production) and have minimized the amount of time that users need to use the physical prototype in dangerous environments. CAVE's are typically used since it is usually desired to see the virtual prototypes in stereo, one-to-one ration, and in first person view.

Haptic stimuli are used in virtual feedback as a result of requiring force feedback in tasks such as assembling, disassembling, or maintenance analysis. Haptics refers to the sense of touch [12]. Virtual Prototyping uses Haptic force-feedback to complete tasks, and many of these devices are arm system inspired from robotics.

The first force feedback haptic device was known as the Aragonne Arm developed by the University of North Carolina within the GROPE System [13]. The Sarcos Dextrous Arm Master was developed shortly after the GROPE System to allow for haptic interaction of virtual objects using the tip of the index finger and the tip of the thumb [14]. The Virtuose 6D35-45

from Haption[1] has also been developed as a haptic arm device. More recently, researchers are looking for ways to increase the reachable workspace for large movement manipulation of virtual objects. The development of these products has revolved around the desire for users to work with a larger workspace in the virtual environment.

2.7 Haptic feedback devices

Large workspace haptic devices have a unique set of requirements. Zinn, Khatib, Roth, and Salisbury developed a list of requirements that large workspace haptic devices must have for proper rendering of virtual objects [15].

To accurately render a virtual object, a haptic device must have the capability to render forces over a large dynamic range, in both frequency and magnitude. The required force output for haptic devices is inversely proportional to frequency. At low frequencies, forces are required to slowly change for actions such as slowly pressing into a virtual object, and at high frequencies, instances of large forces would need to be applied for accurate rending of stiff object such as wall. This also requires that the small amplitude actuator torques must be able to support a high bandwidth system.

A very key aspect of all haptic devices is that they need to be transparent. Transparency is the ability to display zero force to the user of the haptic device over a wide frequency range when the user is not interacting with a virtual object as mentioned by Zinn, Khatib, Roth, and Salisbury. At high frequencies, the effective inertia of the haptic device dominates the

---

1 http://www.haption.com/site/index.html

transparency. At low frequencies, it is friction that dominates the transparency of the haptic device.

It is dangerous to be close to equipment that exhibits a large force on the user. The large workspace haptic device needs a small effective inertia to mitigate any safety concerns of large impact loads that cause injuries.

There has been a major research effort in the field to expand the capabilities of haptic devices. Luecke used an approach to compensate for missing forces of an under-actuated desktop haptic device using a virtual mechanism or "virtual probe." [16] This additionally increased the usefulness of an under-actuated haptic device.

2.8 Teleoperation

Haptics is also often used in teleoperation. Teleoperation refers to operating a piece of equipment or machinery from a remote location. Locomotion in the target environment becomes important, since the user is not in the physical location and a thorough understanding the slave position and orientation is required. The dynamics of the slave and the environment often need to be known beforehand so that a Kalman Estimator may be used to predict the actual signal of the position and orientation of the slave from any noisy measurements [17].

Chapter 3 Related Work

In the field of Virtual Reality, there is much current interest in increasing the reachable workspace for large-scale haptics. It is broadly accepted that in free space the haptic device must be transparent and have negligible frictional forces as well as have minimal inertia, while forces must be stiff when objects are encountered. Mobility and orientation are very important factors in virtual assembly. Mobility is defined as "the ability to travel safely, comfortably, gracefully, and independently," and orientation refers to the ability to situate oneself relative to a frame of reference [18].

3.1 Virtual Locomotion

Much research has gone into increasing the reachable workspace within a virtual environment by way of virtual locomotion. Four techniques have been developed and studied for moving in an immersive environment. Those techniques are the Scaling Technique, the Clutching Technique, the Bubble Technique, and Workspace Drift.

The clutching technique was developed by HAPTION [19]. The clutching technique would let the user use the haptic device as they needed. If at any point the user was uncomfortable due to the positioning of the haptic device, the user could press a button to declutch the virtual cursor from haptic device. The virtual cursor would remain stationary and the user could readjust the haptic device. After the haptic device is stationed, the user can press the button again to re-clutch the device with the virtual cursor and continue working [20].

The scaling technique presented by Vance and Fisher [21] uses a motion amplification technique. The user's motion is limited to the size of the haptic display so a scaling factor is used. The scaling factor is a function of the user workspace and the virtual workspace and is given by the following equation.

$$world\ haptic\ scale = \frac{\max\ workspace\ size}{\max\ virtual\ size} \qquad \text{Eqn. 1}$$

This enables the haptic device to reach the entire span of the virtual space. This enables virtual assembly of large components; however, the limitation is that it is does not directly match the user's movements in the real world to cursor movements in a 1:1 scale.

The scaling technique is an example of position control. Conti and Khatib define different control schemes in spanning large workspaces [22]. Position control is a control paradigm used with computer mice or haptic interfaces. It refers to a mapping in which displacement of the device in physical space directly dictates displacement of the avatar/cursor in virtual space. Ballistic control is a control paradigm that uses a variable scaling factor depending upon the velocity of the haptic device in its workspace. Rate Control is a widely used control strategy. A common form of rate control is a velocity derived abstraction in which displacement of the user object dictates a velocity of the computer object, such as a vehicle or other graphical object displayed on the screen.

The bubble technique is a hybrid position-rate control that visualizes a semi-transparent sphere in the virtual environment [23]. The volume is displayed both visually and haptically. When the cursor is within the bubble, position control is used, once the cursor is outside of the bubble. As the cursor crosses the surface of the bubble, an elastic radial force is experienced. Additionally, rate control is used for relocating the cursor and the bubble visually

when the cursor is outside of the sphere. The equations are depicted below where k is the stiffness, D is the distance between the endpoint of the haptic device, R is the radius of the bubble, and r is the normalized radial vector pointing outside of the bubble.

$$\vec{F} = -k \cdot (D - R) \cdot \vec{r} \qquad \text{Eqn. 2}$$

$$\vec{V} = K \cdot F^3 \cdot \vec{r} = K' \cdot (D - R)^3 \cdot \vec{r} \qquad \text{Eqn. 3}$$

Dominjon then did a comparison of the clutching, scaling, and bubble techniques listed above for using haptic devices with Limited Workspace. The experiment to use for the comparison was a painting task in which participants had to paint selected parts of the virtual model. Post-hoc tests showed that the Bubble and BubbleCam techniques were significantly better appreciated than the scaling and clutching techniques [24].

3.2 Physical Locomotion

Virtual Locomotion does not address the user's need to be able to physically move within a virtual environment. More and more emphasis is being placed on large-scale haptics for use in virtual assembly in automotive and aerospace industries. In many aerospace and automotive virtual assembly processes, the user would need to be able to physically navigate to feel more realistic to the physical scenario. There are a lot of assembly tasks in industry that require an operator to be able to move within his or her work station. A lot of research has been put into how to allow a user to physical navigate the virtual environment by way of physical locomotive interfaces. There are two types of locomotion interface designs that exist today. Treadmill Style locomotion interfaces are based on the redesign of treadmills and stair steppers to provided added flexibility. Programmable Foot Platforms are movable tiles that

realize the locomotion interface in a virtual environment [25]. In any case, the locomotion interface should cancel any motion of the user to enable the user to go anywhere in the virtual environment.

Treadmill Style Locomotion Interfaces were first in development since 1989 [26]. The Virtual Perambulator was the first prototype. The user of the system wore a parachute-like harness and omni-directional roller skate. The motion of the position of the user's feet was measured by an ultrasonic range detector. From the detected motion, the direction and speed of locomotion could be determined and used in the virtual environment. There were two major problems with the Virtual Perambulator. The system's waist belt restricted up-down and turn around motion of the walker's body, and weight and height of the roller skate spoilt natural motion.

The ATR Atlas [27] consists of a motor-powered treadmill on top of a three axis motion platform. With a motion powered treadmill, two major problems present themselves. The developers noted that they needed to determine a way to control the speed of its belt and need to determine a way to control walking direction. The ATR used a position sensor to record the user's toes and waist to represent the walker's body position to record data and utilize it in real-time.

The Torus Treadmill is the next generation of treadmill style locomotion interface developed by Iwata [28]. The design utilizes a torus comprised of a group of belts to enable two directional travel in space.

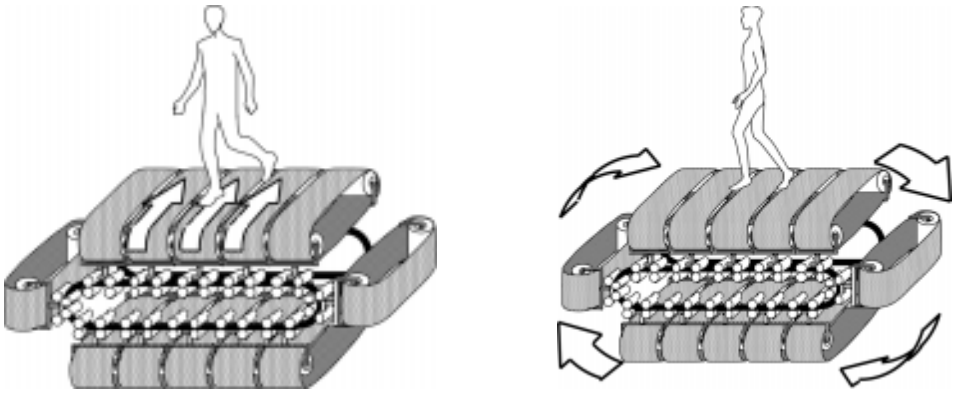

Figure 1: Torus Treadmill directional movements

Additionally, to ensure that the user was centered on the torus treadmill, the knees were tracked to remember the location of the user on the treadmill. There was a circular area on the treadmill that was the insensitive area. If the user stepped outside of the radius of that insensitive area, then the floor would start to move until the user was back in the insensitive area again.

The Sarcos Treadport [29] is a commercial treadmill. The original had a 4-by-8 foot belt area. The second generation had a belt area of 6-by-10 foot. The Sarcos Treadport has the unique capability to tilt to simulate walking on different terrain setting. With such a large belt area, it gives the user the unique capability to use different body postures such as crouching and crawling. This improved the overall maneuverability. The Sarcos Treadport has the unique capability to run at 12 miles per hour and have a peak acceleration of 9.801 meters per second. With the conceptual design, floor projection is also allowed depending on the CAVE configuration. A limitation to this design is the mechanical difficulties the Treadport experiences while turning.

The CirculaFloor [30] is an example of a Programmable Foot Platform. The basic design had the intentions of compact hardware for the creation of infinite surface and scalable hardware architecture for future improvement. The system determined the walking motion of the user by moving proportionally to the user's distance outside of a circular dead zone placed in the center of the walking area. This dead zone prevents over-sensitivity to the user's movements.

3.3 Large-Scale Haptics

Physical Locomotion Interfaces increase the reachable workspace of the user in a virtual environment as well as increases the sensory feedback for the user; however, the current designs that are being researched are not compatible with using haptic devices. This inhibits the user's ability to physically interact with virtual objects. It is very disadvantageous for virtual assembly to not have haptic arm devices to interact with virtual objects because of the depreciation of the tactile feedback without it. Researchers recently have looked into increasing the reachable workspace of haptic devices that would be sufficient for human-scale haptics. That is haptics that fit the majority of tasks needed for majority of human actions or tasks. There currently are four approaches that allow users to have human-scale haptics in CAVE-like environments.

One method for increasing the reachable workspace for human-scale haptics is by using a self-grounded haptic interface that is relied on by tensed cables. It allows the user to walk around freely because the haptic device is worn. Hirose developed a Wearable Force Display called HapticGEAR [31] at the University of Tokyo. In the design of HapticGEAR four design

guidelines were followed. The device weight should be minimized to avoid wearer fatigue. The device should be small and simple to avoid occluding virtual objects visually. The must be safe if it is to be worn on the user's body. The last guideline is that it should be easy to put on or take off. This system does not establish a haptic interface capable of producing enough force. HapticGEAR only produces 2.5 times the force of a Sensable PHANTOM.

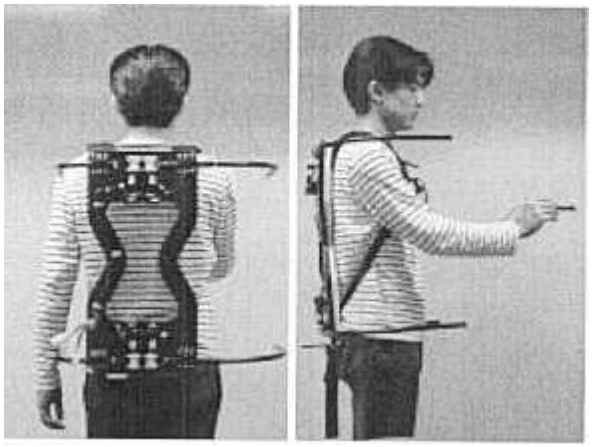

Figure 2: HapticGEAR Exoskeleton

Brau and Gosselin developed the ICARE 3D [32]. ICARE is an acronym for "Interface à Cables à Retour d'Effort." It allows for the user to push through the handle where as HapticGEAR can only pull through the handle because of the configuration. At the current state, it is grounded in order to validate its performance, but the intention is to be mounted onto a wearable structure. The max force considered is 10 Newtons and the max tension allowed is 55 Newtons.

The L-EXOS [33] is a world-grounded wearable haptic interface that is developed for the human arm. It exerts a continuous force of 50 N or a maximum force of 100 N. It is a stationary haptic device that reaches the distance the human user's arm moves. Wearable haptic

interfaces allow for haptic interaction in a CAVE-like environment if it is self-grounded; however, it does not have large force generation unless it is world grounded, which inhibits its capability to simulate virtual assembly with large components.

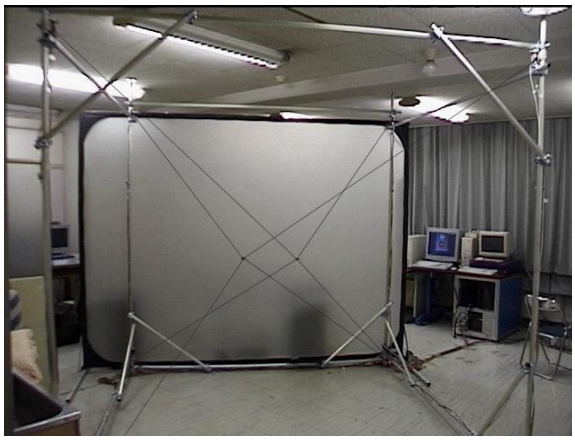

Figure 3: Spidar Tensed Cable Robot

Another approach for having a large workspace for large scale haptics is the use of tensed cable robots. Spidar (SPace Interface Device for Artificial Reality) [34] developed by Ishii and Sato is a stringed force feedback device with various configurations. One allows for three degrees of freedom of force feedback on one point, three degrees of freedom on two points (two fingers from same hand, or one from each hand), or six degrees of freedom of force feedback on one point. The Spidar system is installed on a two-screen workbench, or more generally, a projection-based virtual environment. A novel contribution of the Spidar is the ability to use a mixed prop configuration. This allows for the minimization of the effect of calibration errors due to different positioning of the virtual prop, substituting some parts of the prop with a virtual counterpart for a lighter prop, and allowing the use of generic parts together with virtual parts, that can easily be exchanged. Buoguila, Ishii, and Sato also proposed and implemented a scalable Spidar for increasing the workspace to the size of most CAVE

configurations [35]. Using tensed cable robots debatably needs more research to develop a novel approach to solve the problem of lack of visual occlusion if the mixed prop was behind a virtual component in the virtual environment.

The third approach for increasing the reachable workspace is to use a robot with a redundant axis. Redundant Robots may either be designed or may also be attained by adding a large range axes to an existing haptic device. Gosselin and Andriot developed a large workspace redundant robot using a sliding axis at CEA/LIST [36].

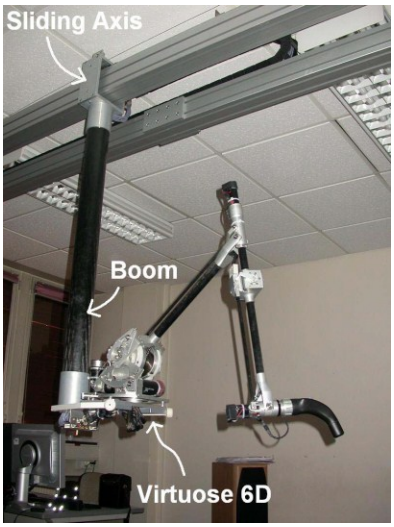

Figure 4: Haption with Redundant Degree of Freedom at CEA/LIST

The force capacity is 24.99 Newtons in continuous operation and 74.7 Newtons peak operation. This allows for a large range of actions that could be done by the user in a virtual assembly process. This also allows for large scale haptics in a CAVE-like environment; however, a significant limitation is not only the cost of a large system, and the inability to transfer the system from one CAVE-like environment to another one.

The fourth approach is to utilize a mobile haptic interface. Mobile haptic interfaces are a mobile robot supporting a haptic device. Mobile haptic interfaces work so that the mobile robot

actively follows the movements of the haptic device [37]. This approach is composed of two systems, the system responsible for control and maintenance of the mobile robot and the system responsible for the haptic interface. The benefits include relative ease-of-transportation in comparison to using a robot with a redundant degree of freedom, as well as including a possible cost reduction. For efficient use, robots with redundant degrees-of-freedom are built for specific CAVE configurations while haptic interfaces mounted on top of a mobile platform can be used in a wide range of configurations and is only limited by the volume of the CAVE configuration. In previous work, Nitzshe, Hanebeck, and Schmidt determined whether a user would be able to identify a virtual wall using a mobile haptic interface [38].

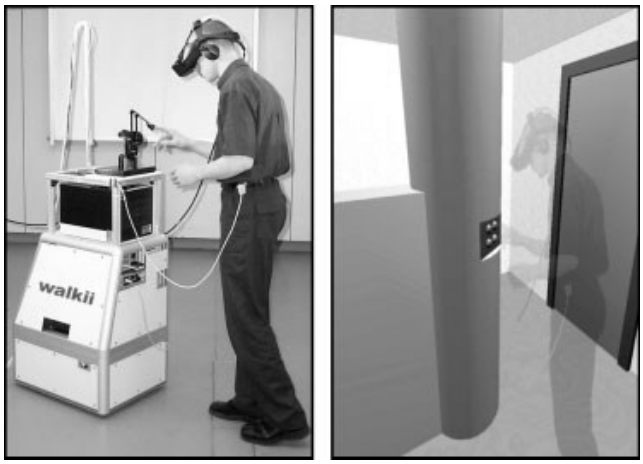

Figure 5: Prototype of Mobile Haptic Interface by Nitzshe, Haneback

Chapter 4 Methods

The goal of the XY table is to keep the haptic device arm displacement as small as possible. This means that even when the haptic device is maintaining a constant force, the XY table moves to center the base under the haptic arm. This will allow the haptic arm device to keep the arm within the force feedback workspace of the haptic device.

4.1 SPARTA

The present work built on the software platform SPARTA, the *Scriptable Platform for Advanced Research and Teaching in Assembly*. This virtual environment allows arbitrary computer aided design models to be loaded and manipulated using haptic force feedback and physically-based modeling. SPARTA is tuned for use of real world units for investigation of interaction in virtual assembly [39]. Pavlik and Vance created the application as the successor to SHARP. SHARP (System for Haptic Assembly & Realistic Prototyping) is a software platform to expand functionality of virtual assembly to include dual handed haptics, swept volume representation, subassembly modeling, and more realistic part behavior [40]. SHARP utilizes VR Juggler and OpenGL-Performer scene graph library for graphical visualization.

SPARTA builds on the VR Juggler open-source virtual reality software framework. All of the graphical visualization is provided by the OpenSceneGraph library that works with VR Juggler. VR Juggler provides a platform for development in virtual reality applications. It serves as a tool to allow researchers to work with simple desktop displays to multi-walled CAVEs [41].

VR JuggLua is an extension of VR Juggler that has scripting capabilities of Lua. It serves as a framework for developing virtual reality applications in Lua. Lua[2] is an embeddable scripting language that allows VRJuggLua to run scripts at run-time. Additional high-level features such as Lua-style creation function of scenes are possible because VR JuggLua takes advantage of the advanced capabilities of Open Scene Graph and VR Juggler [42].

4.2 System Setup

This system is composed of two computers. One computer uses the Windows Operating System and keeps all simulation information up to date and maintains the responsibility of determining and sending the appropriate force for the Phantom Omni to use. SPARTA is the simulation platform for the first computer. The second computer controls the bidirectional robotic platform. The control software requires a real time operating system like Linux Ubuntu while SPARTA is used on Windows. These two computers maintain communication utilizing UDP protocol. UDP is utilized because it is faster than TCP/IP since UDP is connectionless. The flow of information is illustrated in Figure 6.

The numbers in figure 6 correspond to each step in the system flow of information. In step 1, the haptic device sends the displacement of the haptic device arm to the SPARTA simulation software. SPARTA then updates the position of the end-effector and sends it to second computer in step 2. Step 3 entails that the computer responsible for the control of the

---

2 http://www.lua.org/about.html

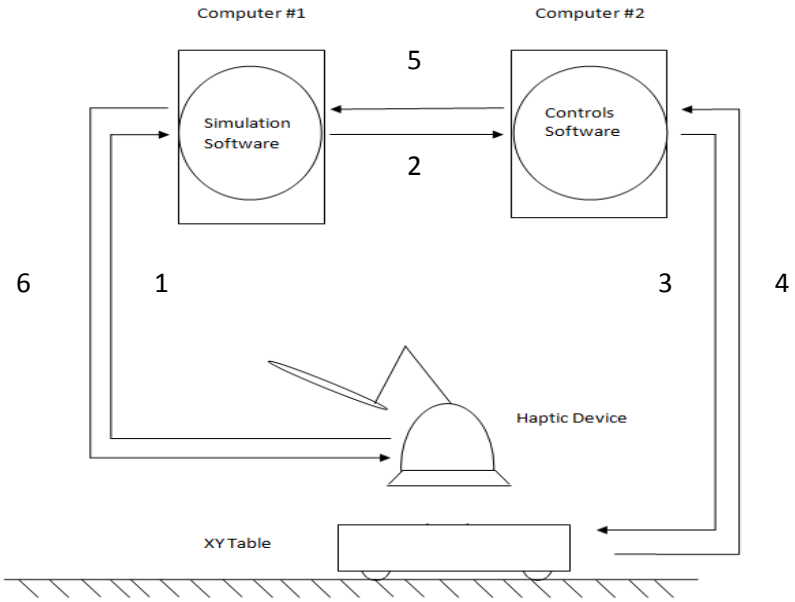

Figure 6: System Flow of Information

XY table receives the position of the end-effector and commands the XY table to move. The XY table sends back its current position back to the control software in step 4. In step 5, the computer responsible for the control of the XY table sends the position of the XY table to the computer maintaining the SPARTA simulation. SPARTA updates the position of the end-effector in the simulation and commands the haptic device to exert a certain amount of force in step 6.

4.3 Control Scheme

The hand inputs to the end-effector of the haptic device. The position of the end-effector relative to the world, x_H, is sent to the XY table. The second computer uses the position of the end-effector and the current position of the XY table to determine the distance that the XY table has to move. The proportional gain is multiplied by the distance that the XY table has to move.

$$V_{in} = K_{P1} x_2 \qquad \text{Eqn. 4}$$

Figure 7 depicts the control schematic for the XY table. K_{P1} (V/m) represents the proportional gain of the XY table in volts per meter. K_T is the motor torque constant for the motor used on the XY table. K_G is the gear ratio from the motor to the XY table. R_m represents the resistance of the motor used and R_g represents the radius of the gear used that moves the chain that moves the XY table in the 2 axes. M_{EQ} and B_{EQ} represent the equivalent mass and damping of the XY table. Laplace transforms where used for the linear differential equations.

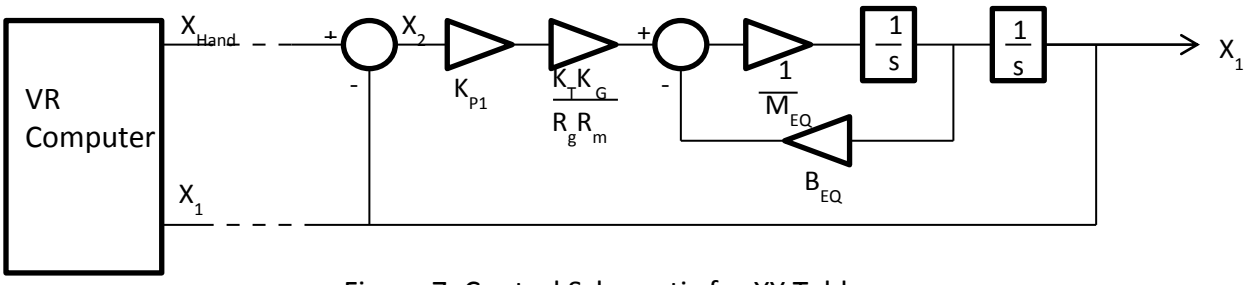

Figure 7: Control Schematic for XY Table

When the distance that the XY table has to move is determined, a proportional gain is multiplied by the distance and is output as a voltage. K_T, K_G, R_m, and R_g take that voltage and convert it into a force in Newtons input to the XY table system dynamics. The output of the XY table is the position, x_1, and is sent back to the VR computer as well as used in the feedback loop for the control scheme.

4.3.1 Movement

For movement, only one direction of motion is considered as the control concept is the same for any linear direction of travel. Figure 8 illustrates the movement of the haptic device and the XY table.

The initial position of the haptic device and XY table are shown in the first step in Figure 8. In the second step, the arm of the haptic device as the end-effector is moved around to interact with the virtual environment. The XY table moves to keep the haptic device arm within the force feedback workspace of the haptic device. The hand inputs to the end-effector of the system and the position of the end-effector is denoted as x_H. The position of the end-effector is the summation of the distance that the arm of the haptic device has moved, x_2, and the distance that the XY table has moved, x_1.

This is how the system will move when the end-effector is in free space of the virtual environment. Free space is when the end-effector is moving and not interacting with any haptic objects in the virtual environment. When the end-effector is interacting with the virtual workspace, the XY table will still move according to figure 8 to keep the haptic device arm in the force-feedback workspace of the haptic device.

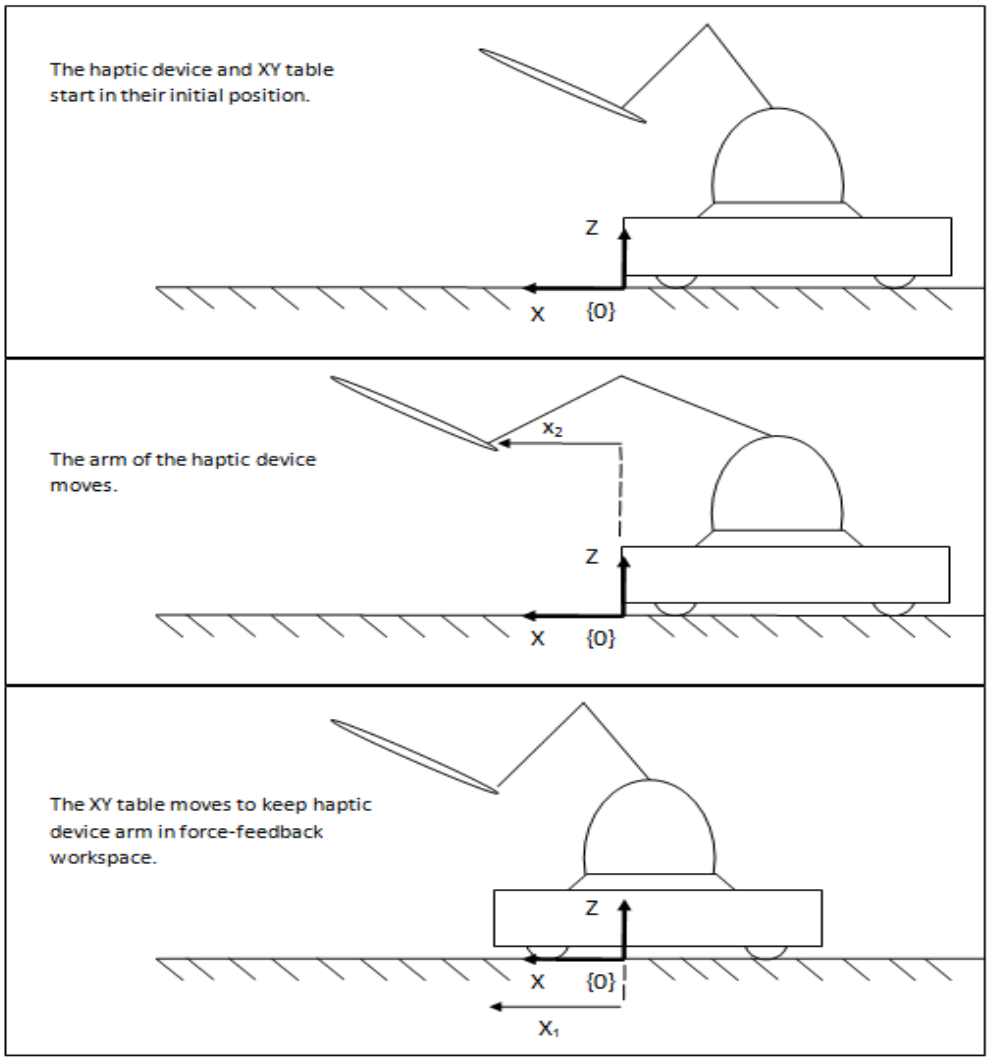

Figure 8: Movement of haptic device with XY table

4.3.2 Virtual Wall

The goal of the movement is to keep the force exerted by the haptic device consistent with the position of the end-effector while the XY table is in motion. A virtual wall is used as the haptic object in the virtual environment because it is simple example of one-dimensional force interaction. The virtual wall will allow the force of the haptic device to be determined while the XY table is in motion.

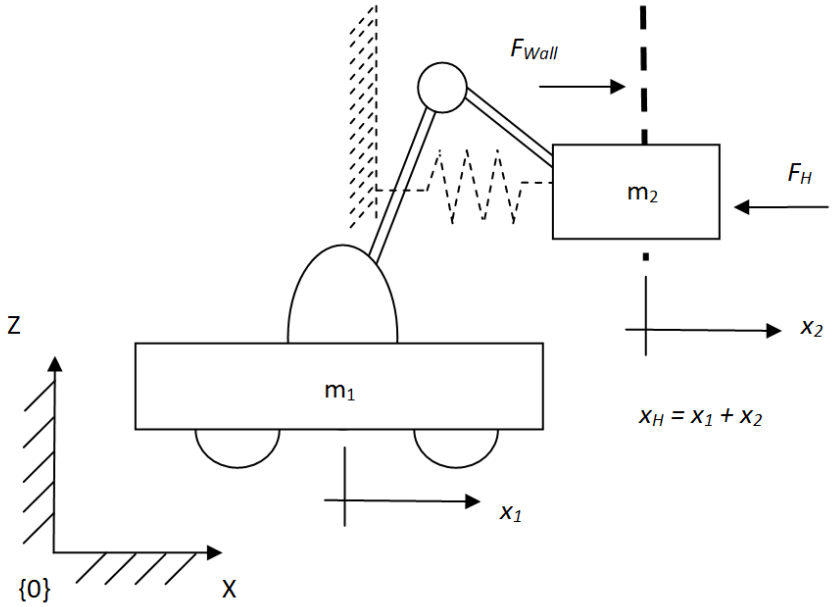

Figure 9: Interaction between haptic device, XY table, and virtual wall

In Figure 9, an illustration of the interaction between the haptic device and XY Table and the virtual wall is shown. F_H represents the force input from the hand to the end-effector of the haptic device. The variable m_1 represents the mass of the XY table platform that is moving and the base of the haptic device. The variable m_2 represents the apparent mass at the end-effector. Haptic arm devices are designed to have a low apparent mass so users do not feel forces due to the weight of the arm during interaction. F_{wall} is the force the virtual wall exerts during interaction. x_H is the position of the end-effector.

The free body diagram for the haptic device is depicted in Figure 10 and the XY Table is depicted in Figure 10. The haptic device is commanded to exert the same force as the virtual wall which is denoted as τ_2.

The XY table was implemented in two dimensions. We will analyze the dynamics for a single dimension. The mass, m2, could also be considered to include the mass of the operator's hand. This example examines the case of hitting a virtual wall in a virtual environment.

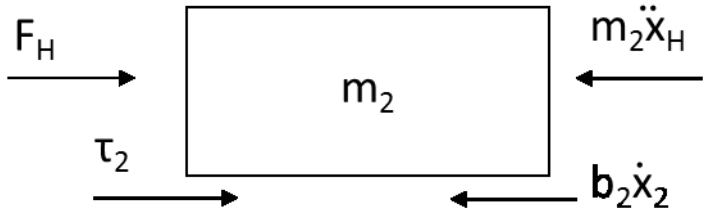

Figure 10: Free body diagram of arm of haptic device

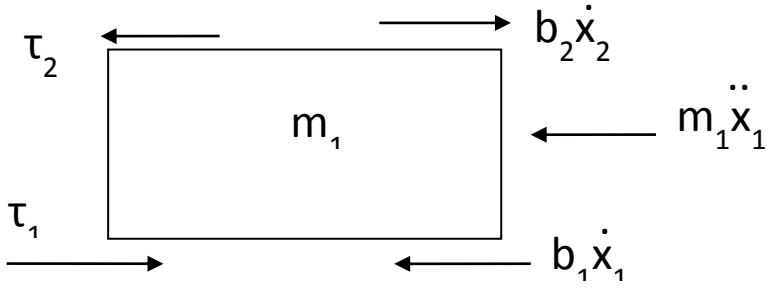

Figure 11: Free body diagram of XY table

From the free body diagrams for the system, the following equations of motions are developed and are shown in Equation 5.

$$\begin{bmatrix} m_1 & 0 \\ m_2 & m_2 \end{bmatrix} \begin{Bmatrix} \ddot{x}_1 \\ \ddot{x}_2 \end{Bmatrix} + \begin{bmatrix} b_1 & b_2 \\ 0 & b_2 \end{bmatrix} \begin{Bmatrix} \dot{x}_1 \\ \dot{x}_2 \end{Bmatrix} = \begin{Bmatrix} \tau_1 - \tau_2 \\ \tau_2 + F_H \end{Bmatrix} \quad \text{Eqn. 5}$$

When the hand hits the virtual wall, the force that the user exerts on the wall at x_H is shown in Equation 6. The force that the user on the wall is depends on how far the user pushes

into the virtual wall and the stiffness of the virtual wall. In free space, the user is not interacting with the virtual wall and should not feel any force which is shown in Equation 7.

$$F_H = -K_E x_H \quad \text{Eqn. 6}$$

$$F_H = 0 \quad \text{Eqn. 7}$$

K_E represents the stiffness of the virtual wall. Ideally, the stiffness of a wall would be infinite, but a varying stiffness is used for force analysis. It would be ideal to simulate an infinite force because in the real world, a human could push on a wall with their maximum force and the wall would push the same force back, but haptic arm devices are physically limited in the amount of force to exert onto the user. The force of the haptic arm device, τ_2, and the XY table force, τ_1, when interacting with the virtual wall are shown in the following equations.

$$\tau_2 = K_E x_{Hand} = K_E(x_1 + x_2) \quad \text{Eqn. 8}$$

$$\tau_1 = K_{p1} x_2 \quad \text{Eqn. 9}$$

In the free motion case, when the user is not interacting with the virtual wall or any other haptic objects in the virtual environment, the forces are shown by Equation 10 and Equation 11. With this implemented, the mobile base follows the position of the haptic device in the virtual environment and still maintains transparency so that the user does not “feel” the additional inertial mass following the user in the virtual environment.

$$\tau_2 = 0 \quad \text{Eqn. 10}$$

$$\tau_1 = K_{p1} x_2 \quad \text{Eqn. 11}$$

For the case when the haptic device interacts with the virtual wall, a relationship can be developed between the position of the base, x_1, and the haptic device arm position, x_2. When the hand is interacting with the virtual wall and the haptic device is not exerting its maximum

force, the position of the base can be written as a function of the position of the haptic device as shown in Equation 12.

$$x_1 = -\frac{K_{p1} + K_E}{K_E} x_2 \qquad \text{Eqn. 12}$$

K_{P1} represents the proportional gain of the XY table to make the XY table move and K_E is the environmental stiffness of the virtual wall. Using Equation 12, functions can be written for the force input by the hand as a function of the position of the base and a function of the position of the haptic device.

$$F_H = -K_{p1} x_2 \qquad \text{Eqn. 13}$$

$$F_H = \frac{K_{p1} K_E}{K_{p1} + K_E} x_1 \qquad \text{Eqn. 14}$$

Equation 13 shows the force that the hand exerts as a function of the position of the haptic device. Equation 4 show that the force of the hand exerts is also written as a function of the position of the base.

4.4 Small-Scale Implementation

A small-scale system was used for experimentation. This provided the opportunity to verify the theory before the implemented on a larger scale. Refer to figure 15.

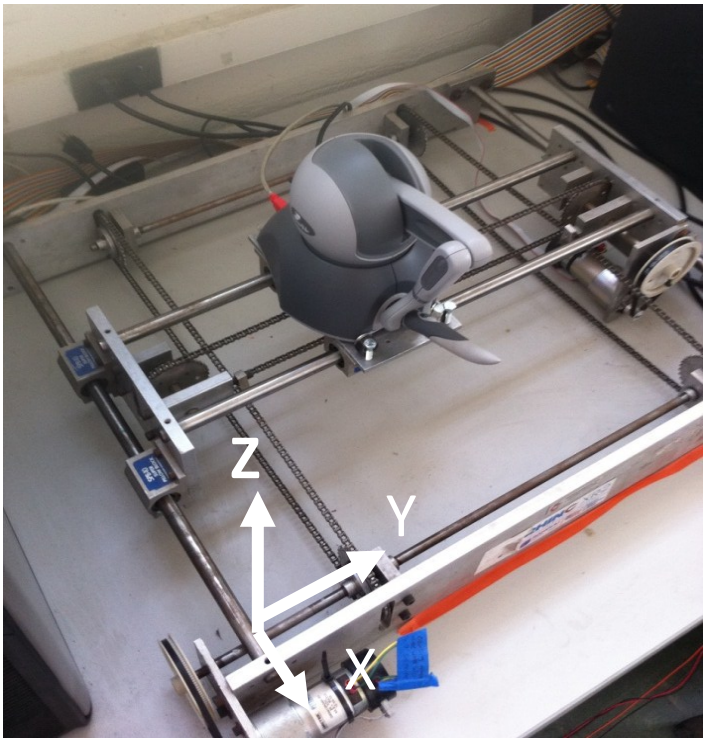

Figure 12: Sensable Phantom Omni with XY motion table

For the small-scale implementation, refer to figure 16 for the distances moved by each body. Figure 16 shows x_2 representing the displacement of the arm of the Sensable Phantom Omni. The distance that the XY table moves the platform is x_1.

4.4.1 Hardware

A Rhino Robotics X-Y Motion table[3] was used as the bidirectional robotic platform for this setup due to availability of resources. The axes are driven by permanent magnet direct-current servo motors. Each motor has an integral gear box with a gear ratio of 65.5 as well as

---

3 http://www.rhinorobotics.com/access2.html

Figure 13: Position of Sensable Phantom Omni and XY table

incremental optical encoders for the measurement of position in real time. The moveable distance or work area of the platform on each axis is 38.1 cm (15 in) in the X axis and 45.72 cm (18 in) in the Y axis. The positional resolution of the XY Table is 0.15mm (0.006 in).The nominal speed of the X-Y Motion Table is 3.81 cm/sec in each direction. An H-bridge was used so that the motor could be driven in either direction. This X-Y Motion Table was controlled using the HAL software available on the Linux Operating System. The voltage sent to the X-Y Motion Table ranged from 0 to 36 Volts.

The Sensable Phantom Omni[4] was selected as the haptic device for this work because of its commercial availability and is a cost-effective haptic device on the market for desktop haptic interaction. It has six degree-of-freedom positional sensing and has a force-feedback workspace

---

4 http://www.sensable.com/haptic-phantom-omni.htm

of 16 cm width, 12 cm height, and 7 cm depth. It exerts a maximum force of 3.3 N (0.75 lb_f) and has force feedback in the x, y, and z directions. It is an impedance controlled device.

4.4.2 Software

HAL[5] (Hardware Abstraction Layer) is a software package that was used as the managing control software for the XY table. It allows components to be loaded and assembled into a complex system using software. It was originally designed for the purpose of configuring variety of hardware devices. The design of HAL resembles how hardware circuits consist of interconnected components. It uses terms such as servo motor, encoder, signal generator, PID controller, and this is particularly useful in terms of the control of the XY table. Majority of HAL components work in real time. Other components of HAL store the data it manages in shared memory so that real-time components can access it when necessary. Based on position of the haptic device, the HAL software sends a pulse width modulated voltage to the XY table ranging as a percentage of 36 Volts.

4.5 Experimental Setup

There are two goals of the study. The first goal is to ensure that the haptic device is exerting the correct force based on the end-effector position while the XY table is moving. The

---

5 http://www.linuxcnc.org/docs/HAL_User_Manual.pdf

second goal is to show that the time for communication between the two computers has a minimal effect on the error of the force commanded by the simulation.

In the study, the user moved the end-effector into free space for a short period of time during stage A. Once the phase of moving in free space was finished, the end-effector then moved to the virtual wall and "tapped" it in the virtual environment in stage B. In stage C, the end-effector was pushed into the wall until the hand was clearly past the surface of the wall. It was then held at that position inside of the wall for an arbitrary amount of time. Then the end-effector is pulled back to the surface of the virtual wall and tapped again in stage D. After tapping the wall for the second time, the haptic interaction with the virtual wall is finished by moving the hand into free space in Stage E. Refer to figure 17.

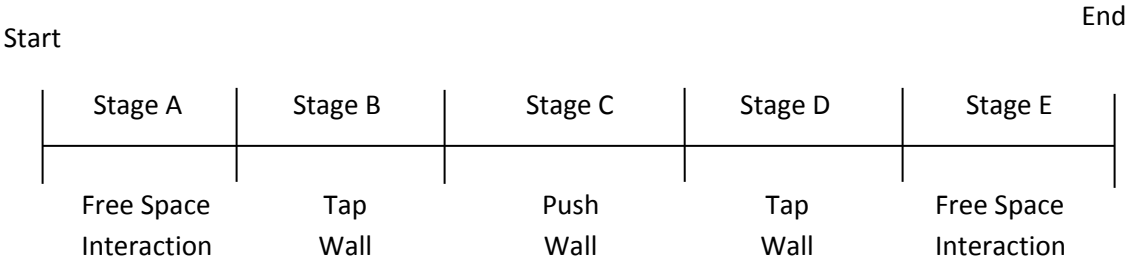

Figure 14: Stages in each trial

Understanding the dynamics of the haptic device with redundant axis is essential for predicting the performance of the system before it is implemented in an immersive environment to evaluate the success of matching the theoretical measurements to the experimental measurements for the XY table, haptic device, and hand position. The experimental data includes the recorded position of the base, x_1, the pulse width modulation signal sent out to the motor (PWM), the recorded position of the end-effector, x_H, the force

sent out to the haptic feedback device, τ_2, and the times for each measurement. A time offset was included so all measurements recorded originated at 0.0 seconds. After the data was recorded, if the first time stamp recorded was non-zero, then the offset was included to make that timestamp equal to 0.0 seconds. The haptic device exerts only a maximum force of 3.3 Newtons (0.75 lb_f). The user was restricted to moving in only one direction, so that results were not affected by movement in two directions.

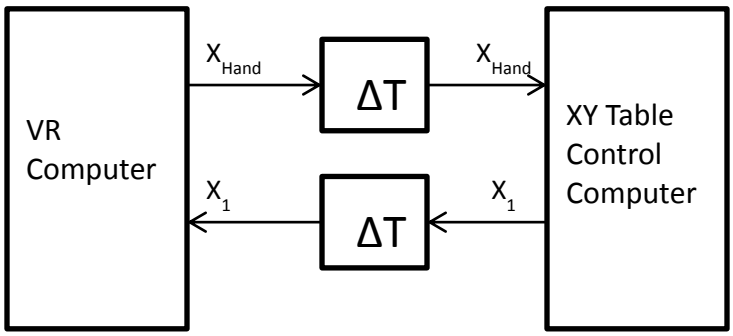

Figure 15: Time delay between two computers

After all trials were taken, it was also desired to see if the time it took to communicate between both computers had an effect on the commanded force of the haptic device. The haptic device force uses the position of the XY table in the previous iteration, while the XY table is still moving. If the measurement from the next iteration is used, then it should be determined whether that latency between the two computers had an effect on the error of the force calculation. This step is done after all data is recorded from the trial.

Chapter 5 Results

The first trial uses low wall stiffness and a high proportional gain for the XY table. Using low wall stiffness in this trial will help us validate that at the point of haptic interaction with the virtual wall, the correct force is being commanded of the haptic device. The second trial uses high wall stiffness and a low proportional gain for the XY table. The XY table will be moving a lot slower than in the first trial as a result of using a low K_{P1} gain. What will be seen is a large movement of the arm of the haptic device before the XY table moves in part due to frictional forces to overcome in addition to the low proportional gain. The last trial uses high wall stiffness and a high proportional gain for the XY table. The last trial would help to identify the error of the force being commanded before the maximum force is exerted by the haptic device.

Table 1 shows all trials that were taken and the parameters for those trials. The second column is the environmental gain that the Sensable Phantom Omni exerts. This is also the stiffness of the virtual wall. The third column is the proportional gain of the XY table in Volts per meter.

Trial	K_E (Newtons/Meter)	K_{p1} (Volts/Meter)
1	80	590
2	800	59
3	800	590

Table 1: Trial Parameters

Each trial has ten figures associated with it. The first figure is a graph of the position of the XY table, x_1, position of the haptic device arm, x_2, position of the end-effector, x_H, and the force of the haptic device, τ_2, divided by the environmental gain, K_E. If the haptic device is exerting the correct force, then when the force is divided by the environmental stiffness, it should overlap with the position of the end-effector when interacting with the virtual wall. The position of the end-effector is the summation of the position of the XY table and the position of the haptic device arm. The position of the virtual wall is 0.0 meters.

The second, third, fourth, fifth, and sixth figures show the positions of the XY table, x_1, position of the haptic device arm, x_2, position of the end-effector, x_H, and the force of the haptic device, τ_2, divided by the environmental gain, K_E for each stage in each trial. The seventh and eighth figures show the figure illustrate the force based on the position of the end-effector and equation 8, the force the haptic device exerted during the trial given the position of the end-effector, and the force that would be exerted if the position of the XY table from the next iteration is used. The ninth and tenth figures show the error of the force during the trial.

Trial 1: K_E = 80 N/m K_{P1}= 590 V/m

The goal of trial 1 is to look at the case of using a high proportional gain for the XY table and low wall stiffness. With low wall stiffness, the penetration into the wall will be larger before the haptic device exerts its maximum force. That allows the researchers to see the force being commanded by the haptic device matches the end-effector position over a larger range of end-effector positions in comparison to using high wall stiffness.

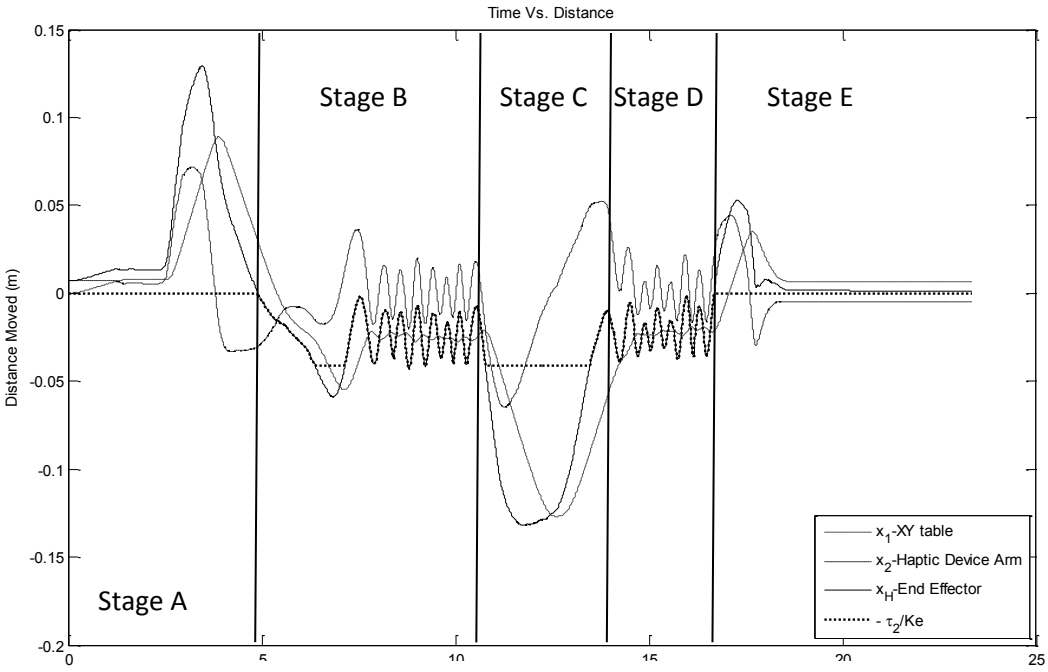

Figure 16: Position of haptic device arm, XY table, and end-effector for K_E = 80N/m K_{P1} =590 V/m

In figure 16, the stages of each trial can be seen. In stage A, the end-effector pushes into the wall before being moved into free space. Since the end-effector is in free space, the force of the haptic device is at 0.0 Newtons and this is also seen in stage E. Stage B and stage D are seen in figure 18 and figure 20 as a result of seeing the oscillatory motion of the end-effector as the wall is tapped. Stage C, when the end-effector pushes into the wall, the maximum force is being exerted by the haptic device even though the XY table is still moving. By including stage D and stage E, the distinctive characteristic for each task can be validated since the task is done more than once.

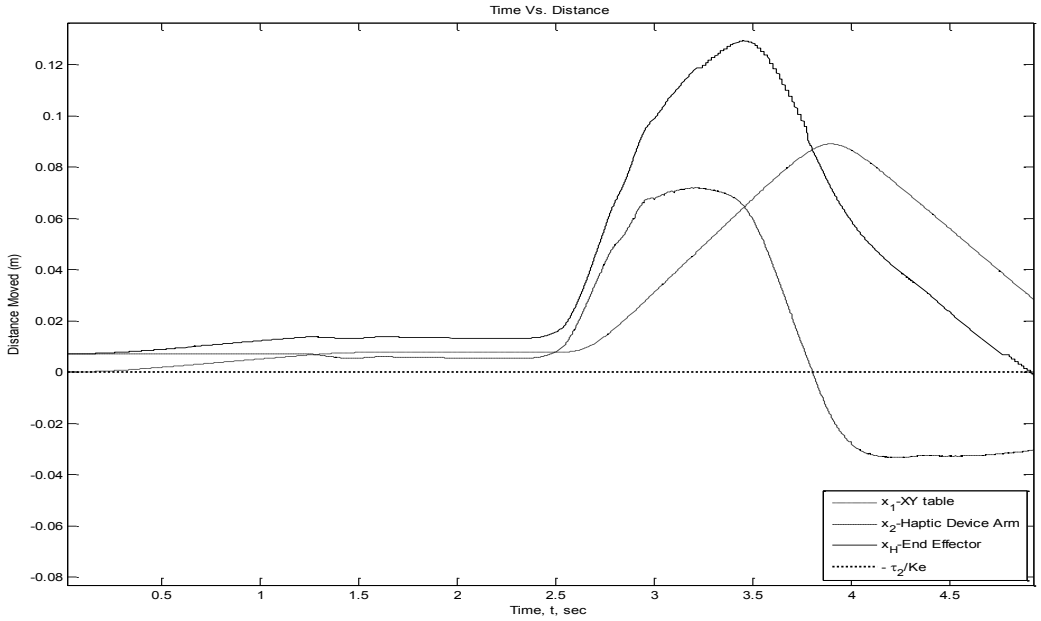

Figure 17: Stage A for K_E = 80N/m & K_{P1} = 590 V/m

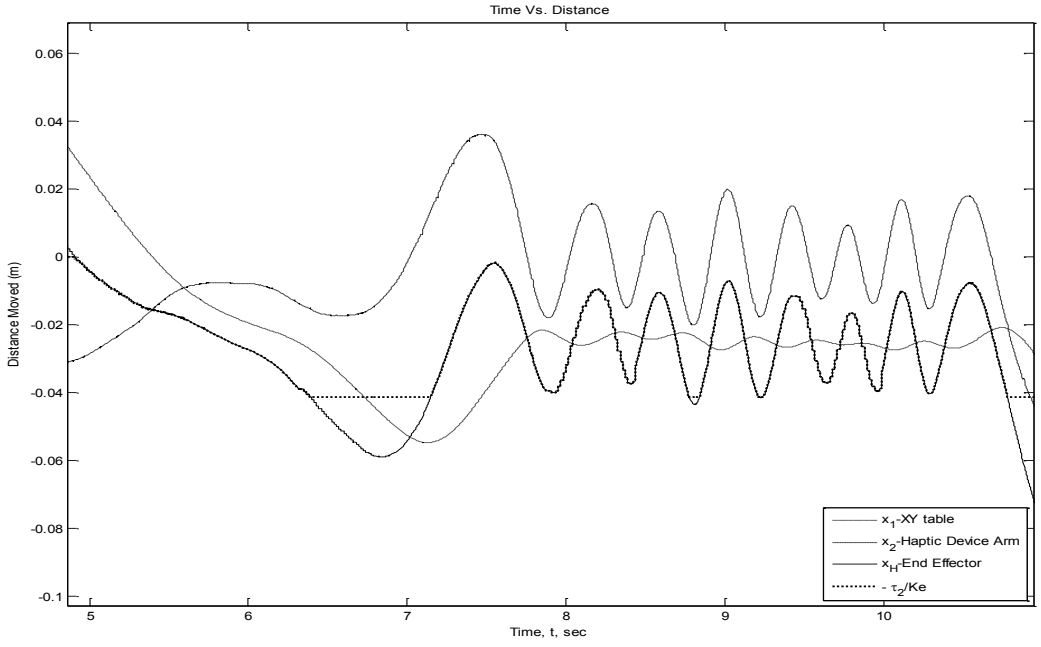

Figure 18: Stage B for K_E = 80N/m & K_{P1} = 590 V/m

In figure 17, stage A shows that the haptic device is not exerting any force and that the position of the end-effector is in free space. The position of the end-effector is not equal to or less than 0.0 meters which is the location of the virtual wall. Figure 18 shows at the point of time the end-effector hits the virtual wall, the haptic device exerts the commanded force while the XY table is moving until the force needed by the simulation exceeds the maximum force of the haptic device.

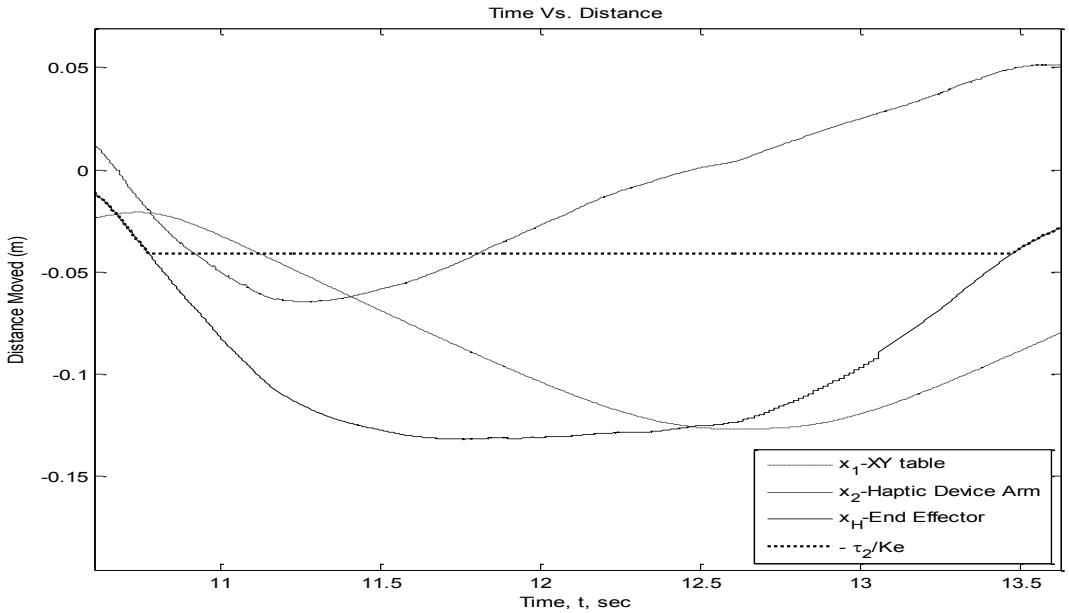

Figure 19: Stage C for K_E = 80N/m & K_{P1} = 590 V/m

Stage C in figure 19 is the task of pushing the end-effector into the wall. The maximum force output occurs at 0.04125 meters depth into the wall coinciding with the maximum force of the haptic device divided by the wall stiffness. The end-effector continues to push further into the wall and the haptic device exerts a constant force as if a virtual wall is there.

Figure 20 illustrates stage D and has a similar oscillation as in stage B because it is the same task as in stage B. The force of the haptic device divided by the stiffness of the wall is matches the position of the end-effector signifying the haptic device force is not exerting the maximum force output.

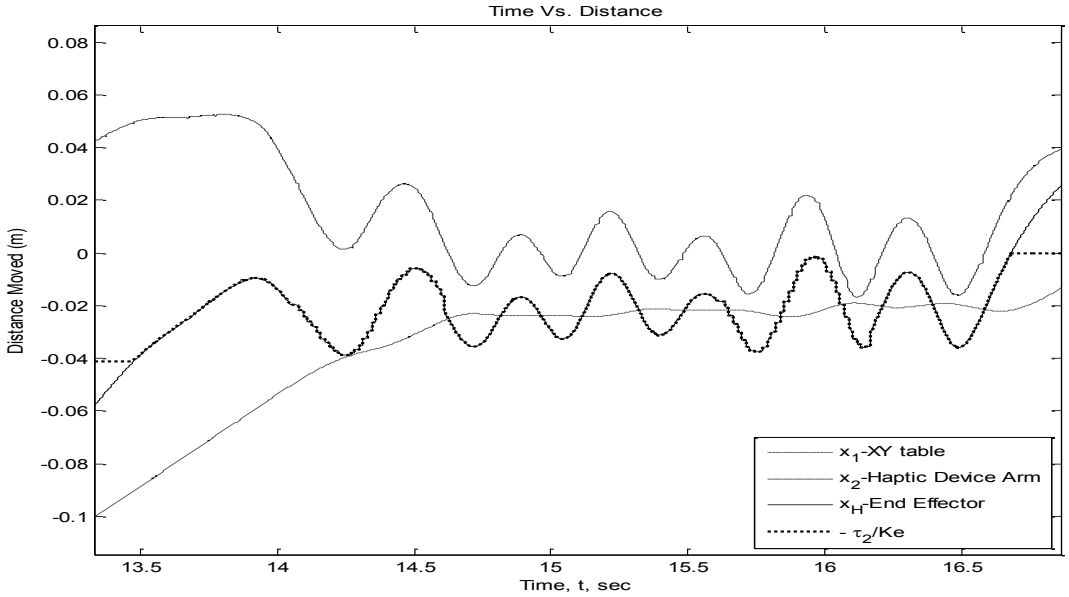

Figure 20: Stage D for K_E = 80N/m & K_{P1} = 590 V/m

In figure 21, the end-effector is brought into free space and the haptic device does not exert any force on the end-effector. This is the same as stage A, which is also the end-effector moving in free space. The XY table is still following the movement of the arm of the haptic device in stage E.

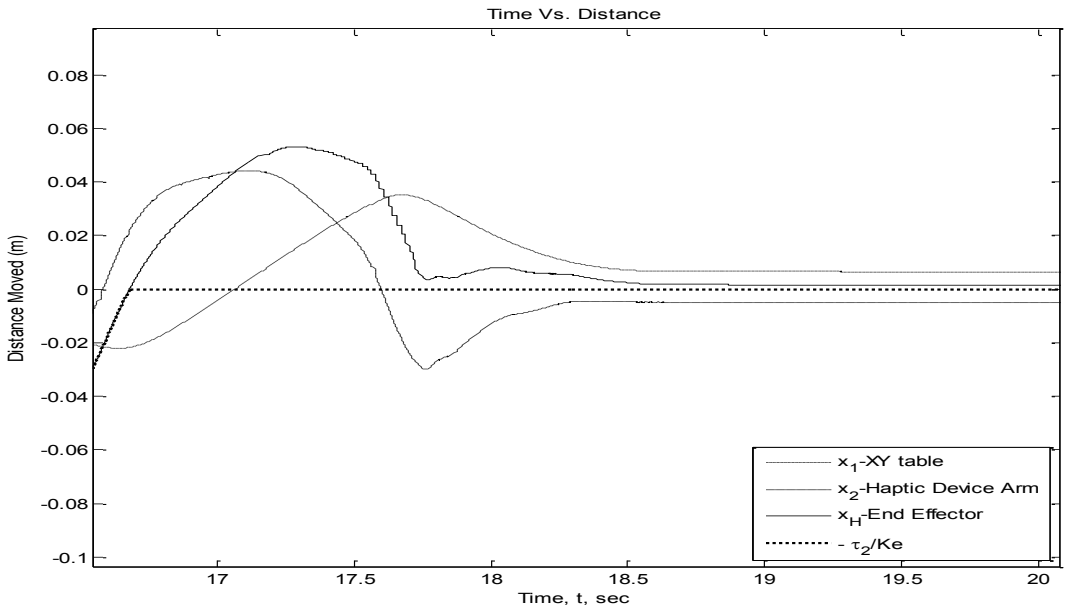

Figure 21: Stage E for K_E = 80N/m & K_{P1} = 590 V/m

In figure 22, the force exerted by the haptic device is shown as a function of the position of the end-effector. Equation 8 is shown in figure 22, and if the correct force is being exerted by the haptic device, then τ_2 and $K_E \bullet x_H$ should overlap each other as long as the haptic device is not exerting any force or producing the maximum force output. τ_2' is the force that would be exerted by the haptic device if the measurement of the XY table, x_1, is used from the next iteration. This can only be known after all data from the trial is recorded.

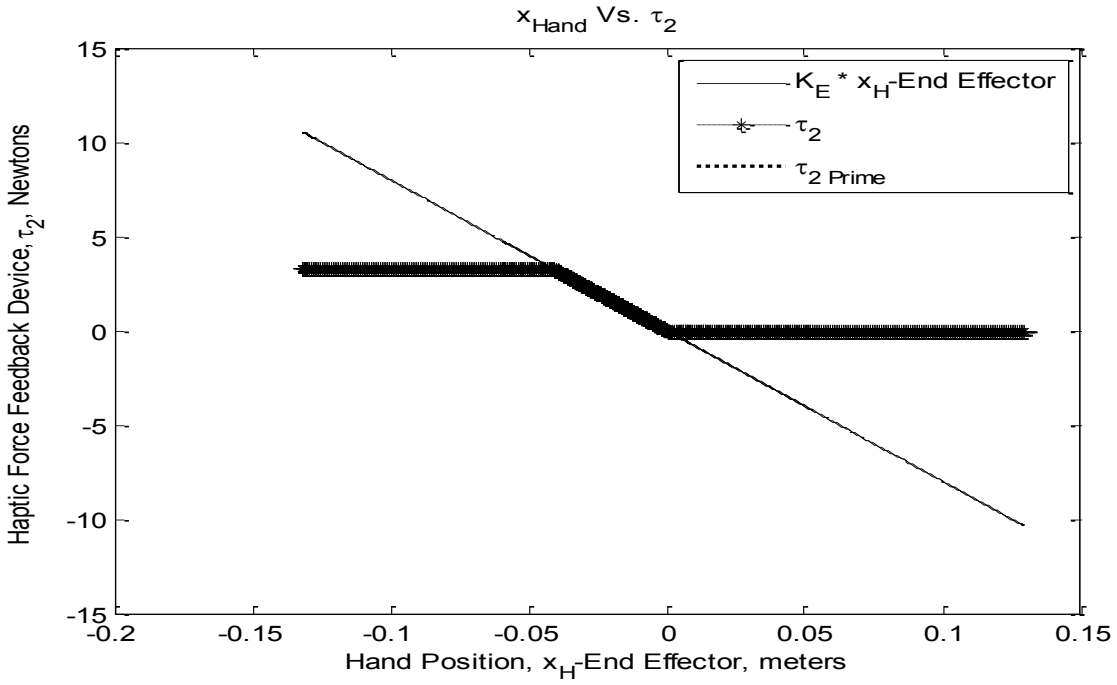

Figure 22: Force of Haptic device vs. end-effector position for
K_E = 80N/m K_{P1} =590 V/m

In figure 22, the difference between τ_2 and τ_2' is indistinguishable, so figure 23 shows a small region of figure 22. The region is close to the point the haptic device is exerting no force and when the haptic device begins to interact with the virtual wall. After zooming in on figure 22 for figure 23, the difference between τ_2 and τ_2' is really small. That means for this trial, the latency between the two computers does not have a visible difference.

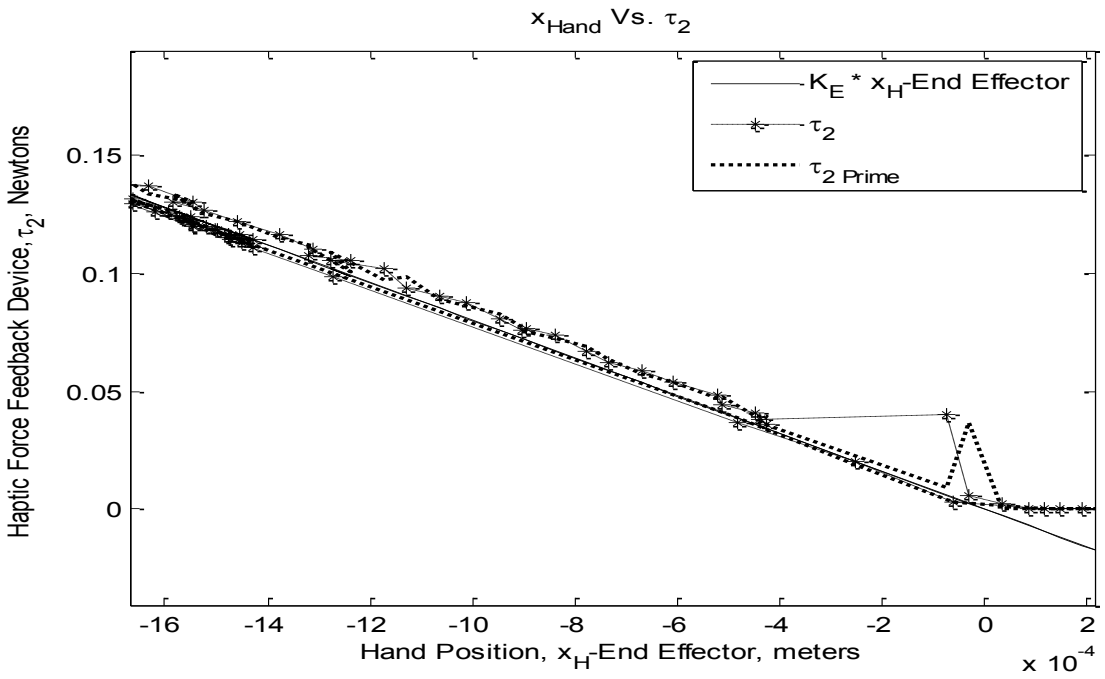

Figure 23: Close-Up of haptic device force vs. end-effector position for K_F = 80N/m K_{P1} =590 V/m

In figure 24, the error of the force is shown as a function as time. The peaks of the error in the figure are due to the limitations of the force output of the haptic device. The most prominent peak from the time of approximately 11 seconds to 13 seconds corresponds to the stage C of the trial. As the end-effector pushes farther into the wall, the force that is commanded of the haptic device is higher, but the haptic device is limited to 3.3 Newtons. There is a large error of force in the beginning because the end-effector pushed into the wall

briefly before being pulled into free-space where no force should be exerted.

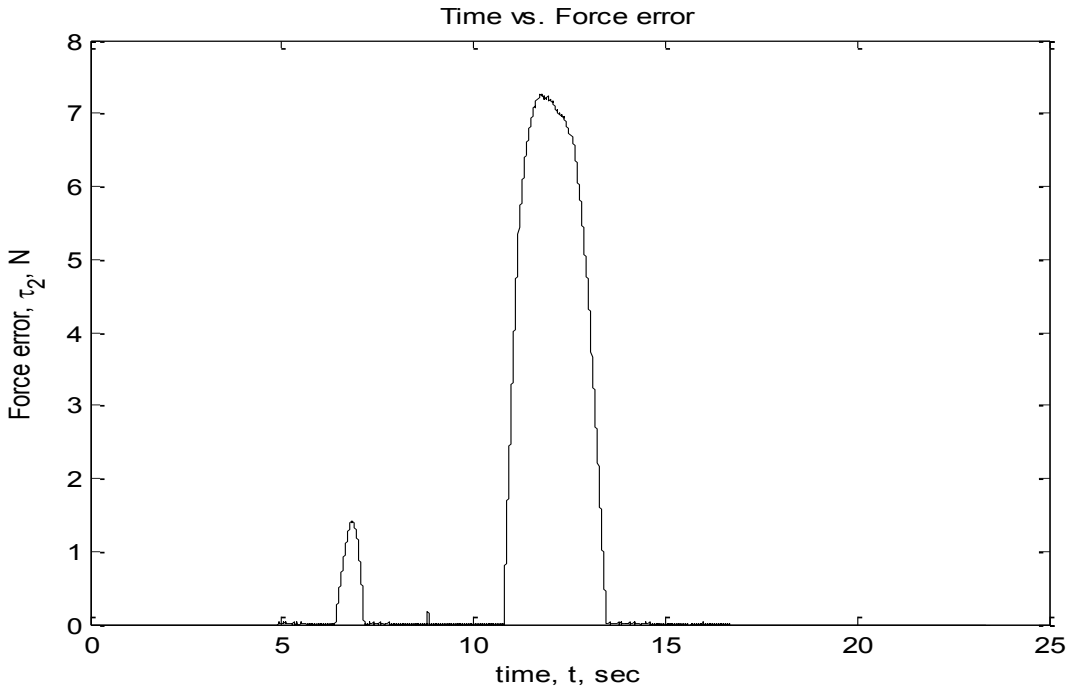

Figure 24: Error of haptic device force as a function
of time for K_F = 80N/m K_{P1} =590 V/m

It is also desired to look at the error force when the force of the haptic device is able to render the force called by the simulation. As a result, figure 245 shows a small region is figure 24 that corresponds to stage B when the end-effector is tapping the wall. The majority of the measurements have an error less than 0.01 Newtons.

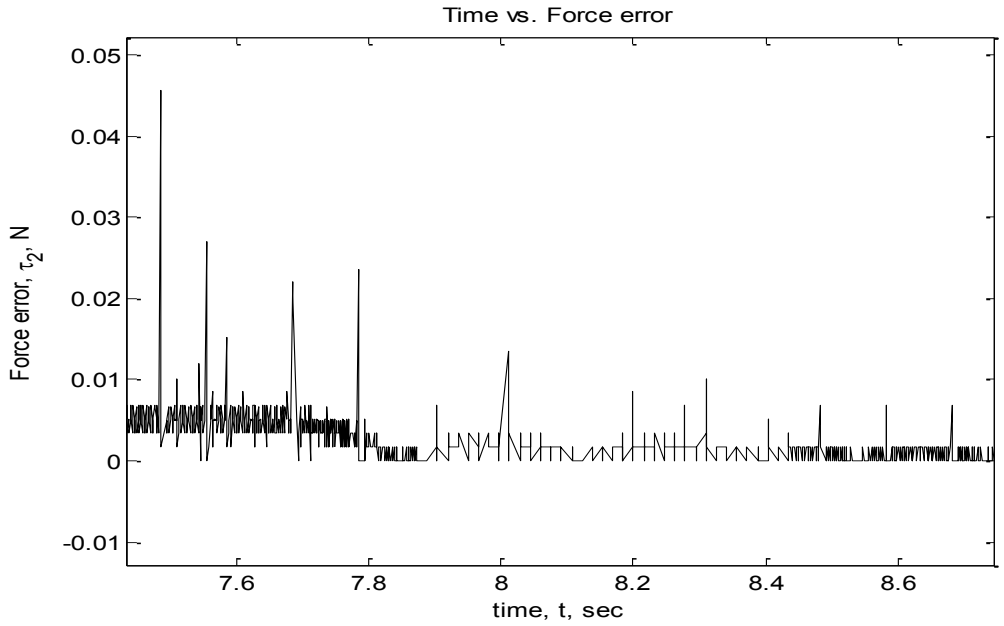

Figure 25: Haptic device force error vs. time during stage B
for K_E = 80N/m K_{P1} =590 V/m

Trial 2: K_E = 800 N/m K_{P1}= 59 V/m

Trial 2 uses high wall stiffness and low proportional gain for the XY table. This trial shows that the arm of the haptic device will have to move a larger displacement for the XY table to follow the position of the haptic device arm. In trial 1, the force commanded was shown to match the end-effector position, so in trial 2 the high wall stiffness can be used. This gives a smaller depth into the wall before the maximum force is exerted by the haptic device. This is desired in order for it to feel like a virtual wall.

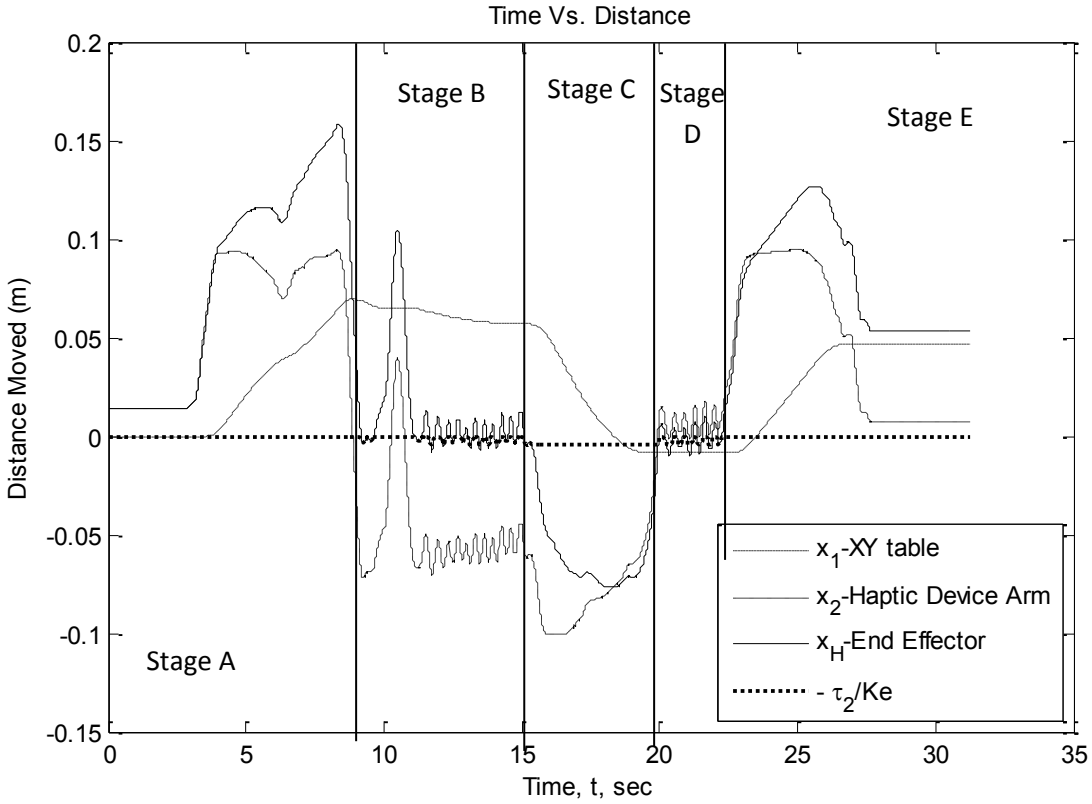

Figure 26: Position of haptic device, XY table, and hand for K_E = 800 N/m K_{P1} =59 V/m

Figure 26 shows the positions of the XY table, haptic device arm, end-effector, and the force of the haptic device divided by environmental stiffness for every stage during the trial. Because a lower proportional gain is used for the XY table, a much slower response is seen for the position of the XY table.

In figure 27, the arm of the haptic device moves a displacement of 10 centimeters in stage A before the XY table follows the movement of the arm. The position of the end-effector is limited in how far it can move into free-space due to the XY table. This can be seen because the haptic device arm displacement is constant, close to its maximum reachable workspace and the slope of the position of the haptic device matches the slope of the position of the XY table.

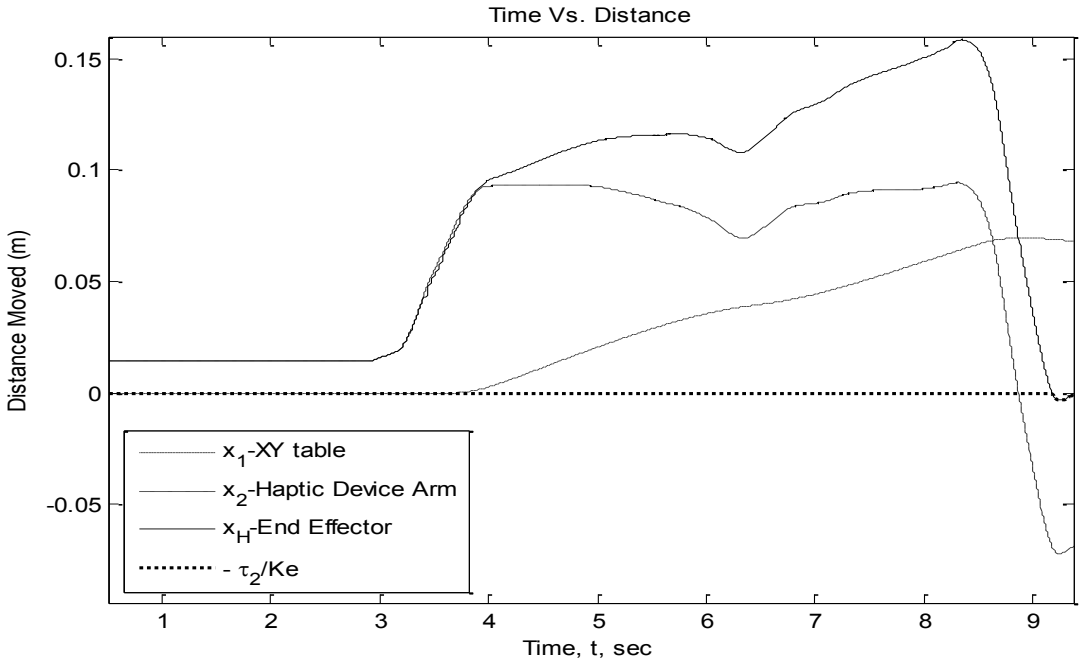

Figure 27: Stage A for K_E = 800 N/m & K_{P1} = 59 V/m

Stage B of trial 2 is illustrated in figure 28. When the end-effector taps the wall, the end-effector pushes into the wall a distance of 0.004125 meters before the haptic device is exerting the maximum amount of force. When the haptic device does not have to exert a force larger than it is capable of producing, the force exerted matches the position of the end-effector.

Figure 29 shows stage C of trial 2. The haptic device is exerting a constant force while the XY table is moving. As the end-effector pushes farther and farther into the virtual wall, the haptic device force does not change because it is already producing the maximum force output.

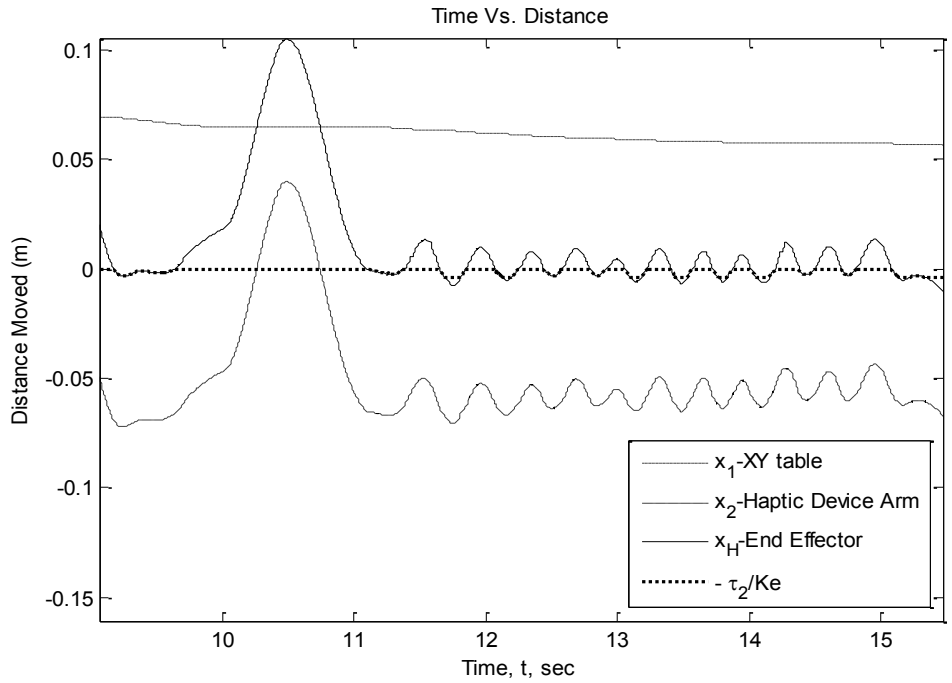

Figure 28: Stage B for K_E = 800 N/m & K_{P1} = 59 V/m

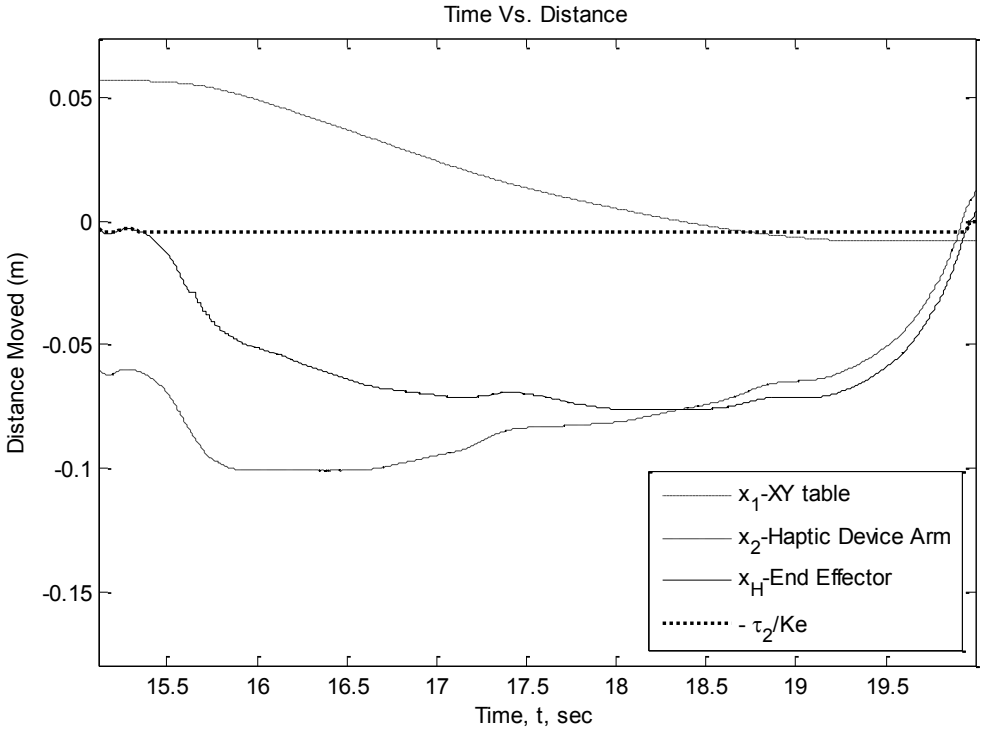

Figure 29: Stage C for K_E = 800 N/m & K_{P1} = 59 V/m

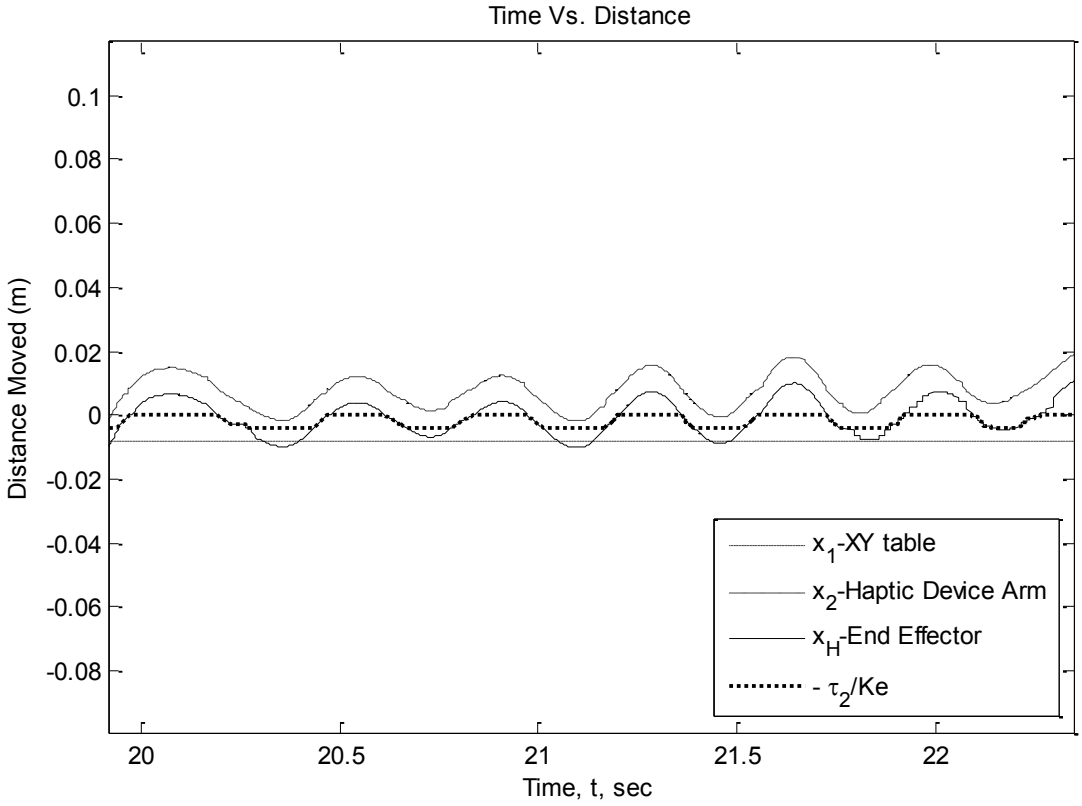

Figure 30: Stage D for K_E = 800 N/m & K_{P1} = 59 V/m

Stage D is shown in figure 30. When moving from pushing into the wall to tapping the wall, the haptic device arm has a positive displacement and the XY table still has a negative displacement, this is opposite of stage B when moving from free space to tapping the wall. In stage B, the XY table had a positive position while the haptic device arm had a negative position. In both cases, the end-effector is still at the virtual wall. If the haptic device arm has a negative displacement, then the XY table will have a positive position during interaction with the virtual wall.

Figure 31 depicts stage E of trial 2. The end-effector moves into free space away from the virtual wall and the force exerted by the haptic device is 0.

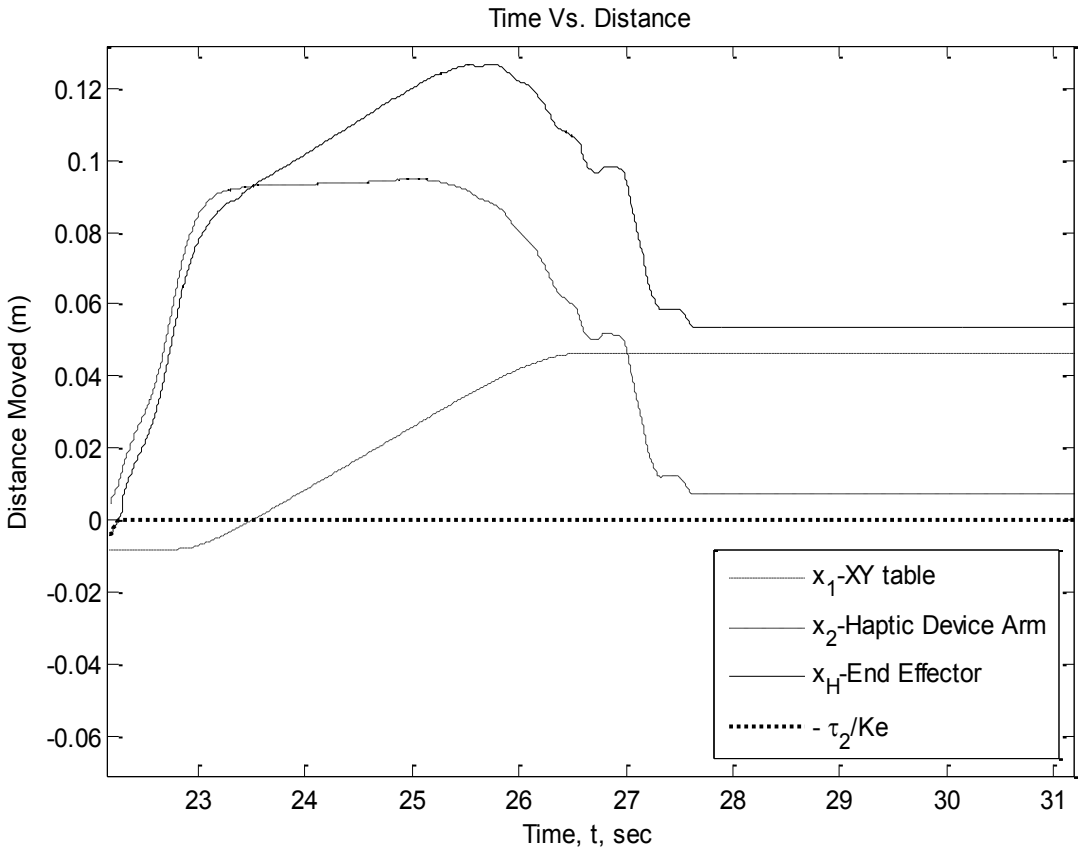

Figure 31: Stage E for K_E = 800 N/m & K_{P1} = 59 V/m

Figure 32 and figure 33 are depictions of the force exerted by the haptic device as a function of the end-effector position for trial 2. By looking at figure 32, the difference between τ_2 and τ_2' is indistinguishable so a closer look at the position of the end-effector when the haptic device starts to exert force shows that the two values still really close to each other given the position of the XY table from the next iteration. The latency between the two computers shows no significant effect in response.

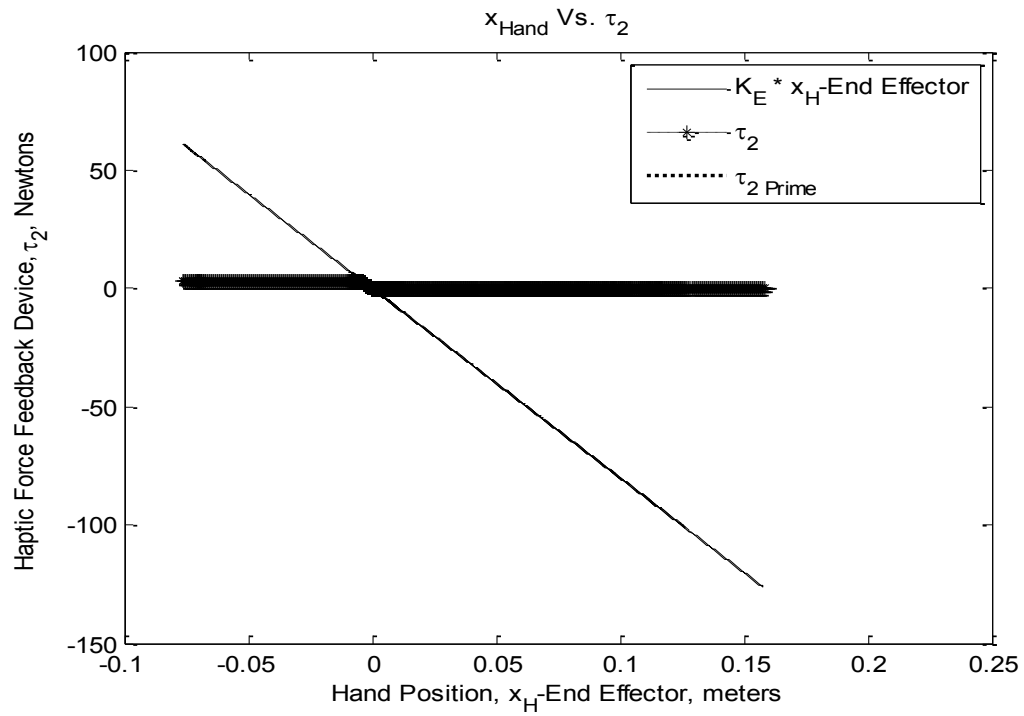

Figure 32: Force of Haptic device vs. end-effector position for K_E = 800 N/m K_{P1} =59 V/m

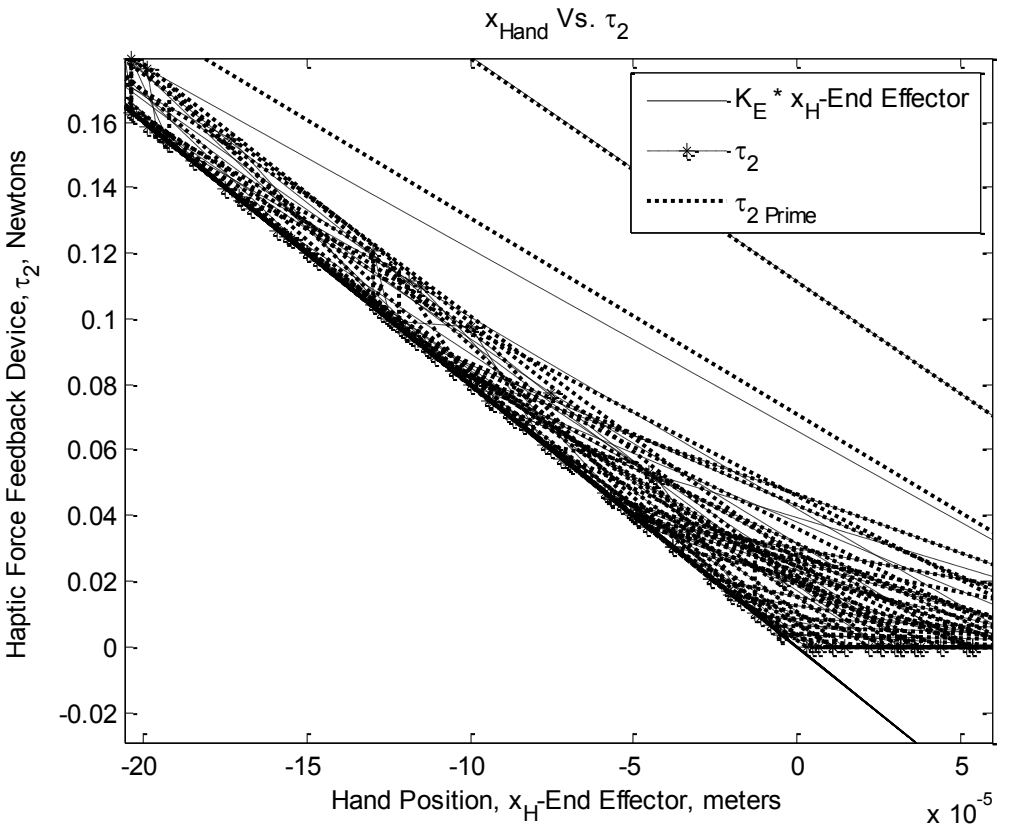

Figure 33: Close-Up of haptic device force vs. end-effector position for K_E = 800 N/m K_{P1} =59 V/m

The error of the haptic device force is shown in figure 34. Doing a comparison between the error of the force in trial 1 (refer to figure 24) and trial 2, shows that the magnitude of the in trial 2 is larger than the previous trial. This is a reflection of the magnitude of the wall stiffness between trial 1 and trial 2 is 10.

For figure 35, a portion of figure 34 was used that corresponded to when the end-effector "tapped" the wall and the haptic device could render the force without producing the maximum force output. The error does not exceed 0.02 Newtons when the haptic device is able to produce the force called.

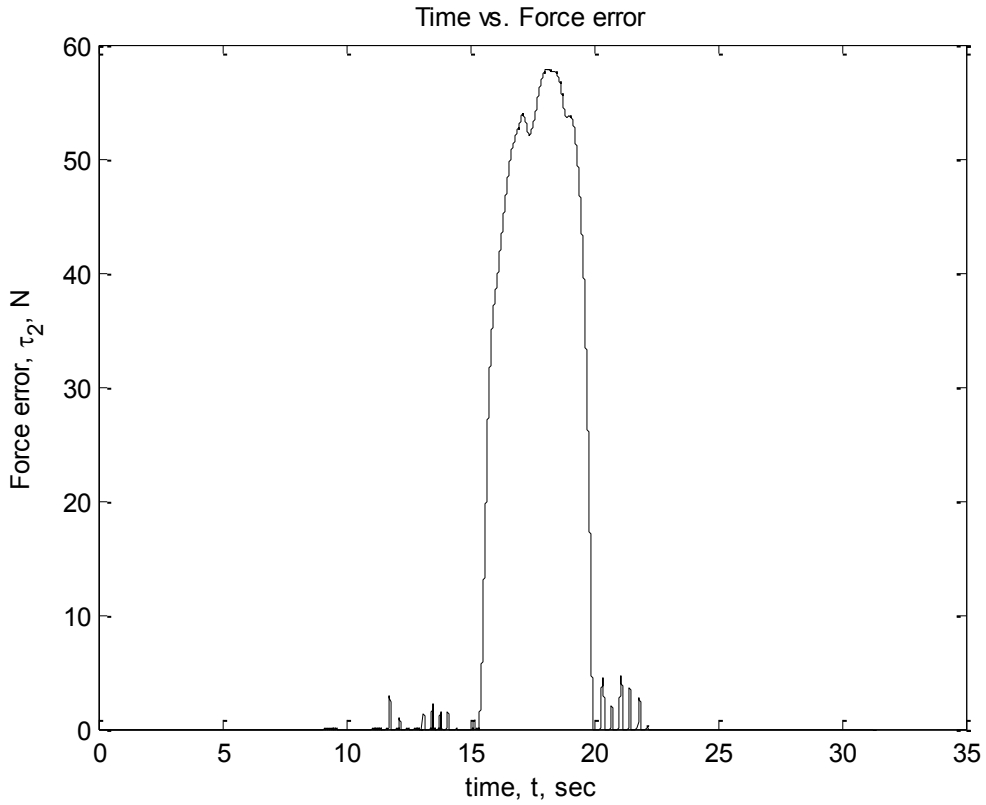

Figure 34: Error of haptic device force as a function of time for K_F = 800 N/m K_{P1} =59 V/m

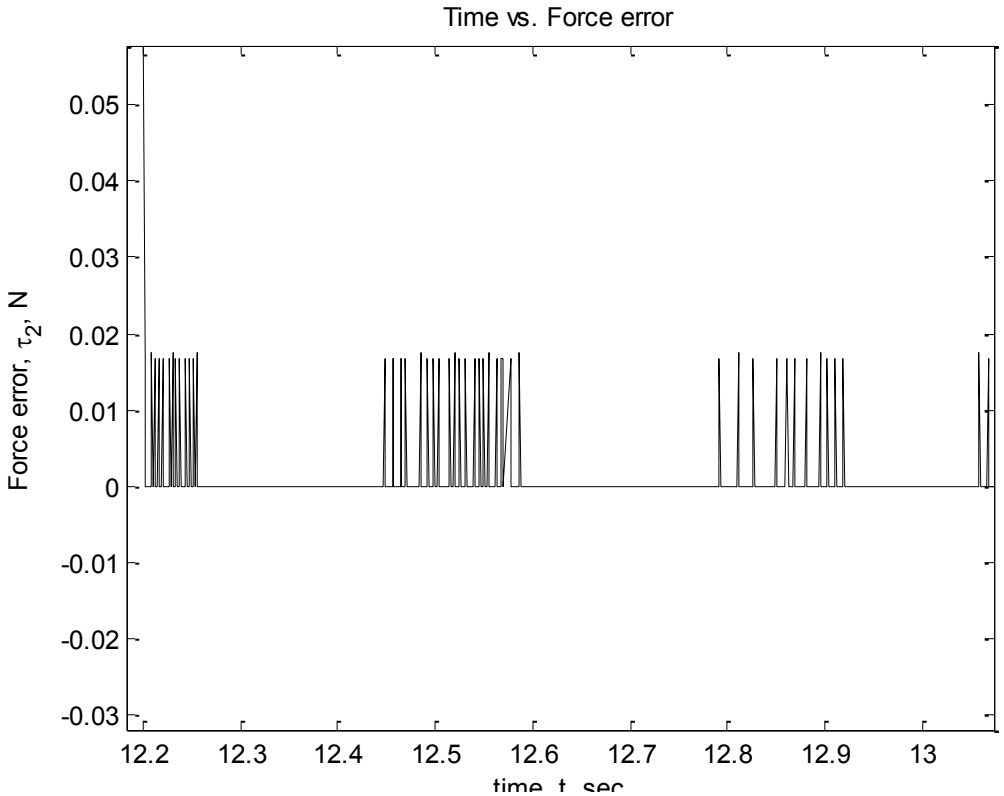

Figure 35: Haptic device force error vs. time during stage B for K_E = 80N/m K_{P1} =590 V/m

Trial 3: K_E = 800N/m K_{P1}= 590 V/m

This trial has a high environmental stiffness of the virtual wall. This trial is expected to have the highest error as a result of having both high wall stiffness and high proportional gain for the XY table. Trial 3 has the same depth as trial 2 that the end-effector pushes into the wall when the haptic device produces the maximum force output. This is important because it is desired to have the virtual wall "feel" the same independent of how fast the XY table moves. This trial shows the XY table has an improved response in keeping the arm of the haptic device within the force-feedback workspace, so that the haptic device arm does not have to reach its maximum reach before the XY table moves as in trial 2.

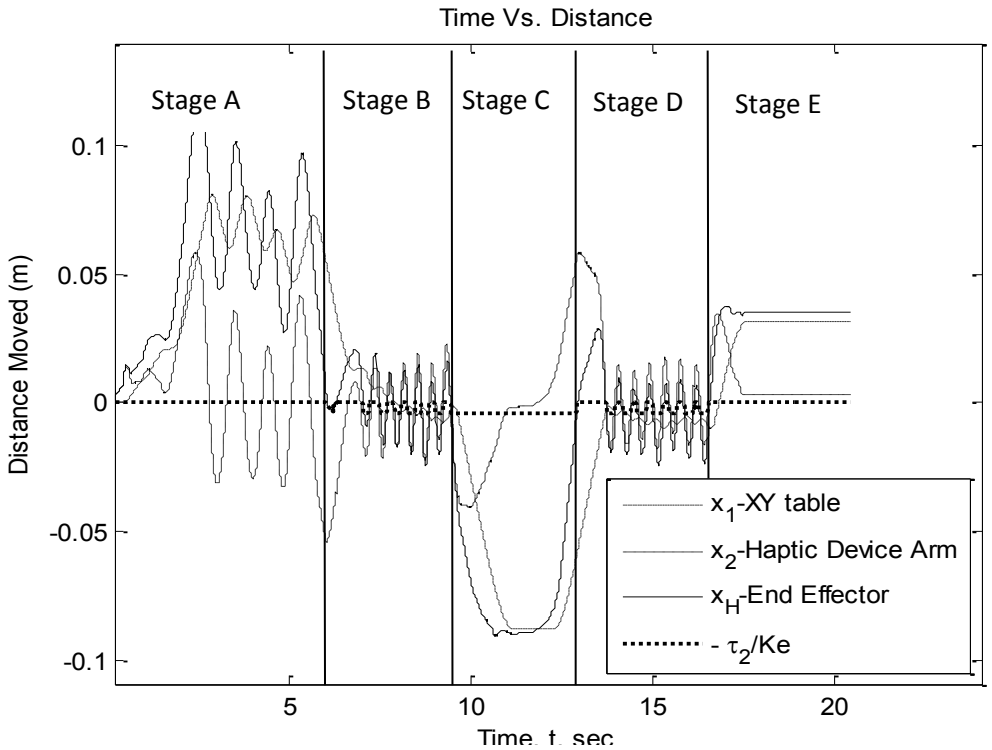

Figure 36: Position of haptic device, XY table, and hand for K_E = 800 N/m
K_{P1} =590 V/m

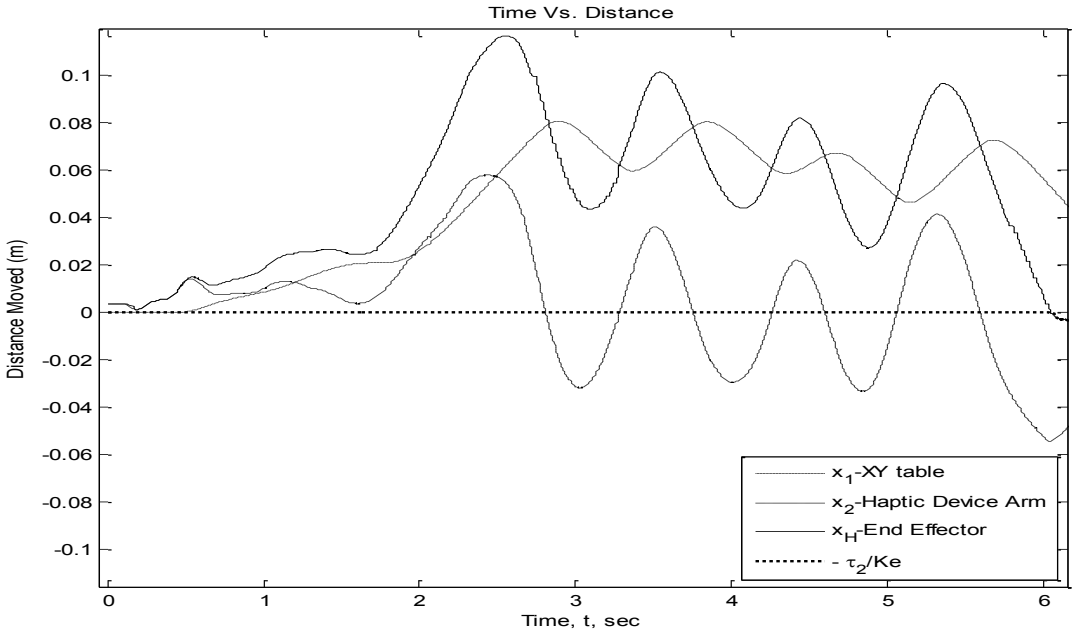

Figure 37: Stage A for K_E = 800 N/m & K_{P1} = 590 V/m

In figure 36, the position of the XY table, haptic device arm, end-effector, and the force of the haptic device divided by the environmental stiffness are shown for the entire trial. Figure 37 illustrates is stage A of trial 2 and no force is applied by the haptic device until the end-effector comes into contact with the virtual wall. Stage B is illustrated in figure 38. When tapping the virtual wall, the force exerted by the haptic device divided by the wall stiffness matches the end-effector position as long as the haptic device is not producing its maximum force output. The end-effector pushes into the wall a distance of 0.004125 meters when the haptic device is producing the maximum force output. This is the same depth as trial 2 while in trial 3, the XY table has a higher proportional gain.

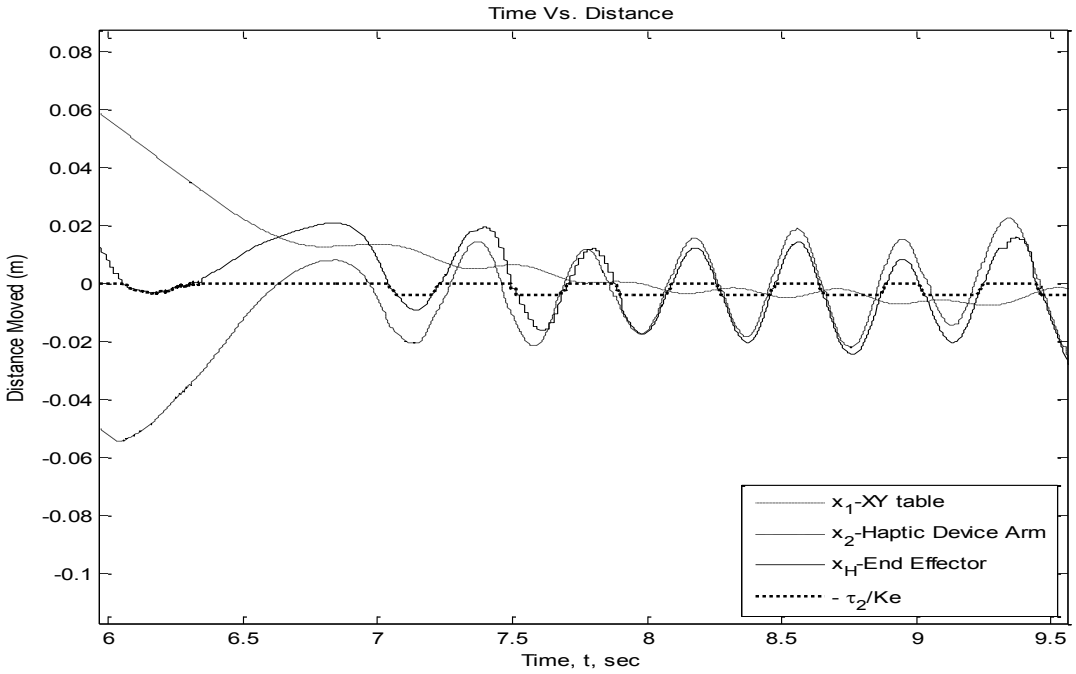

Figure 38: Stage B for K_E = 800 N/m & K_{P1} = 590 V/m

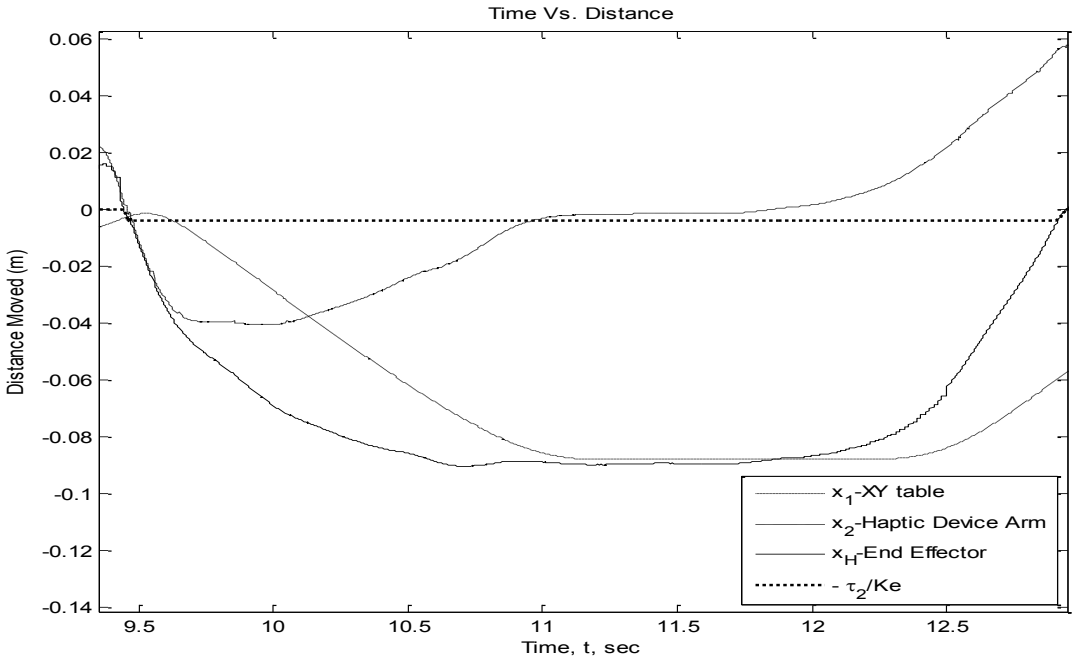

Figure 39: Stage C for K_E = 800 N/m & K_{P1} = 590 V/m

Figure 39 is stage C of trial 3. The haptic device is exerting a constant force when the end-effector is pushed into the wall at a minimum depth of 0.004125 meters. The end-effector is pushed into the wall past a depth 0.05 meters. This is because the hand was able to produce more than the maximum force of the haptic device. The XY table is still moving while the force produced by the haptic device is constant.

Figure 40 illustrates stage D of trial 3 when the user moves from pushing the end-effector into the wall to tapping the wall. The haptic device arm has a positive displacement and the XY table has a negative position while the end-effector is interacting with the virtual wall at 0.0 meters.

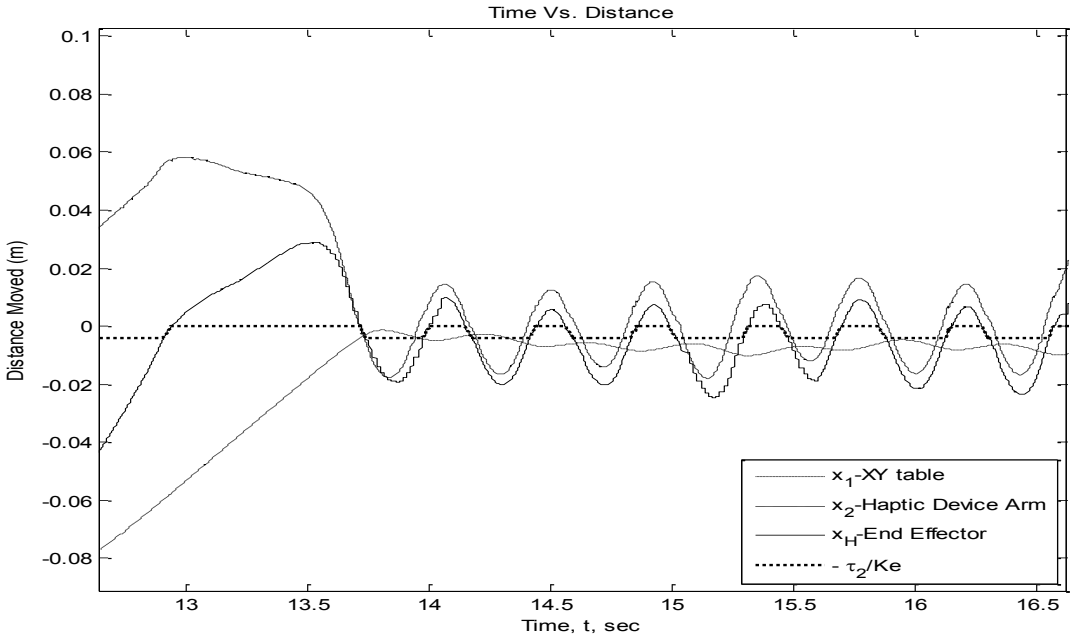

Figure 40: Stage D for K_E = 800 N/m & K_{P1} = 590 V/m

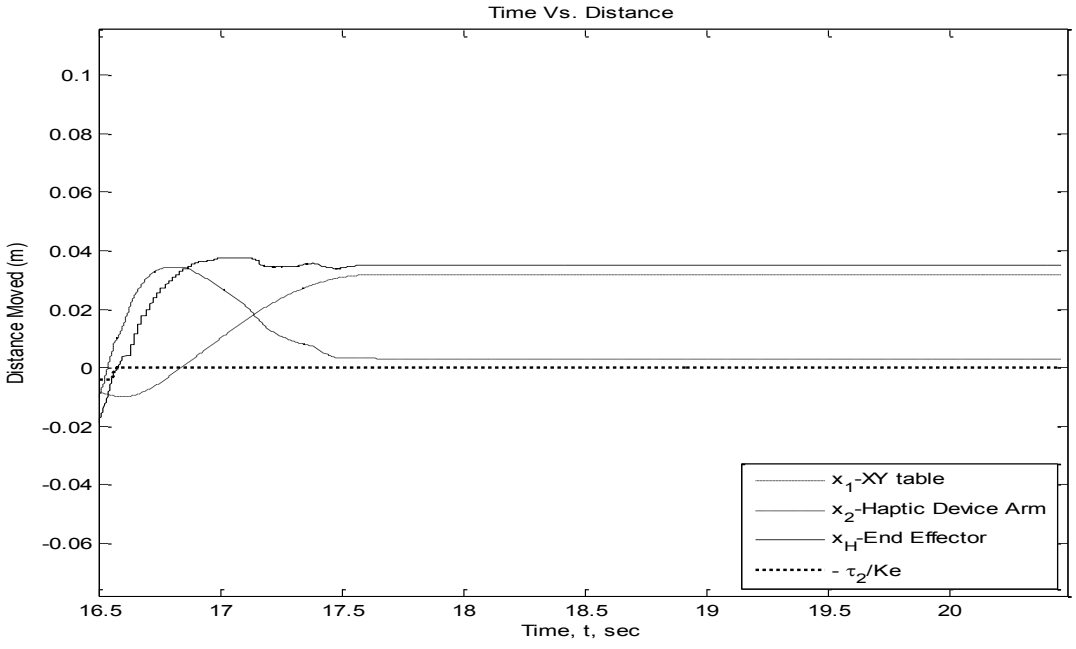

Figure 41: Stage E for K_E = 800 N/m & K_{P1} = 590 V/m

Figure 41 shows the end-effector moving into free space. As the haptic device arm moves in the positive direction, the XY table moves to keep the displacement of the haptic device arm within the force feedback workspace even though the haptic device does not need to apply force in free space. No force is applied by the haptic device in figure 41.

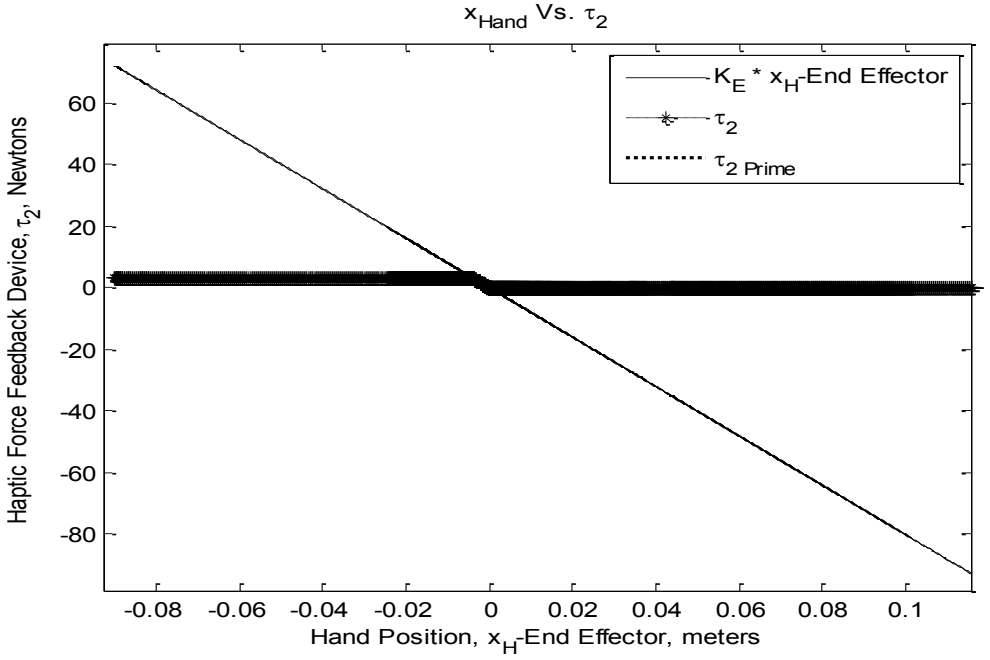

Figure 42: Force of Haptic device vs. end-effector position at
K_E=800N/m and K_{P1} =590 V/m

Figure 42 illustrates the force commanded of the haptic device as a function of the end-effector position. It includes the force of the haptic device during the trail, the force that would be exerted if x_1 from the next iteration is used, and the force that should be used given the equation of the force of the virtual wall. Figure 42 shows the small region of figure 41 when the haptic device begins to exert force when the end-effector reaches the position of the virtual wall. By looking at figure 43, τ_2 and τ_2' are very close to each other in value, so the latency between both computers used in the system has little effect on the force exerted by the haptic device.

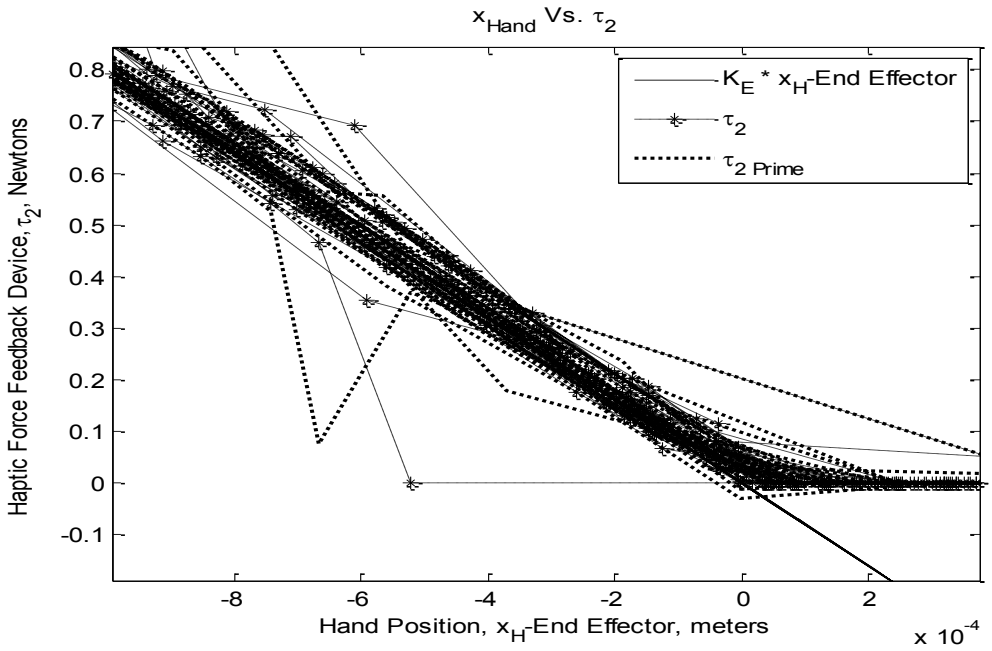

Figure 43: Close-Up of haptic device force vs. end-effector position at K_E = 800 N/m and K_{P1} =590 V/m

Figure 44 shows the error of the force over the entire trial. All of the peaks are due to the haptic device not being able to produce the force needed for the wall because the haptic device is exerting its maximum force. Figure 45 shows the error of the force when the haptic device is not producing its maximum force output. The majority of measurements are well beneath 0.05 Newtons between 7.2 seconds to 7.5 seconds. A comparable weight is the holding two U.S. standard pennies. This is small compared to the weight of a human adult's hand. This force is small compared to the weight of the user's hand that is used to input force into the end-effector of the haptic device.

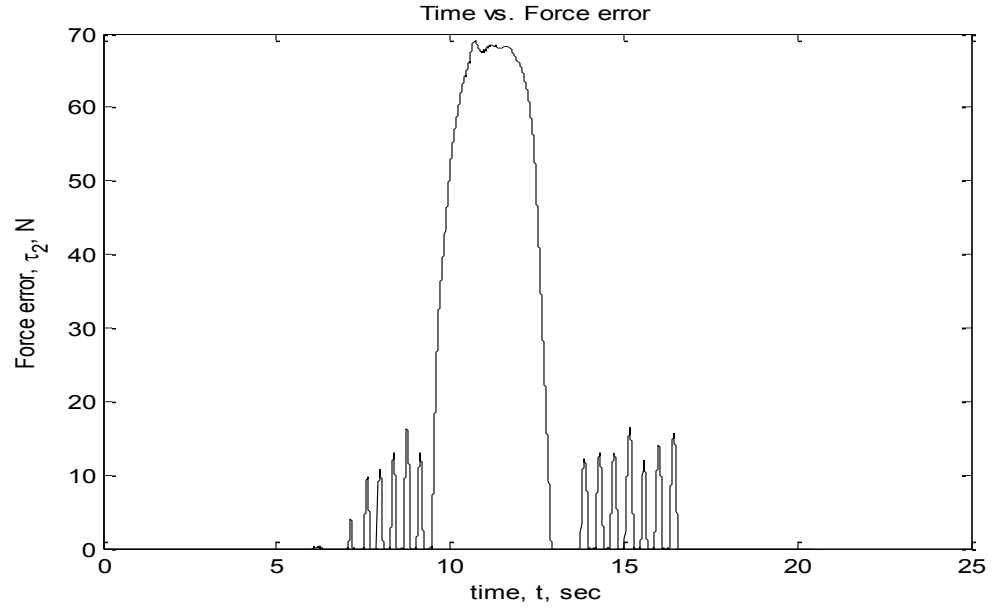

Figure 44: Error of haptic device force vs. desired force output at K_E= 800 N/m and K_{P1} =590 V/m

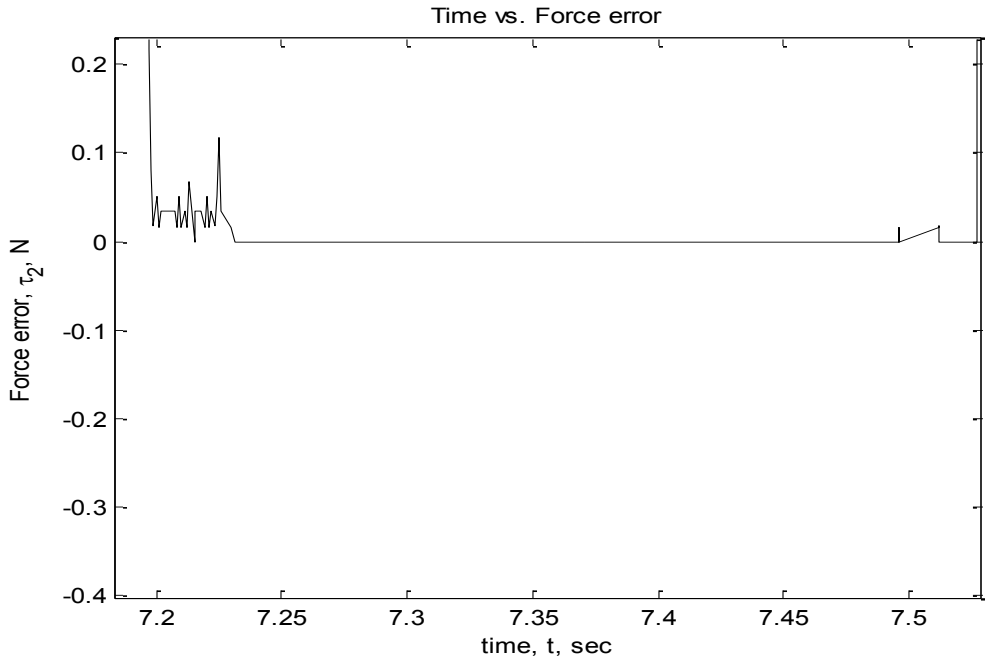

Figure 45: Error of haptic device force vs. desired force output at K_E = 800 N/m and K_{P1} =590 V/m

Chapter 6 Discussion and Conclusion

Previously, researchers identified desirable conditions for large workspace haptic devices. In this work, a method was employed that increased the usefulness of a commercial-off-the-shelf haptic device and increased the reachable work space of the haptic device for a desktop virtual reality application.

In this work, a haptic device with a redundant axis was examined to look at the force feedback on the hand as the XY table moved. This research work identifies that the force exerted on the user's hand matches the force of the virtual wall even though the XY table is moving beneath the haptic device. This work uses a haptic device with redundant degrees of freedom and works within the SPARTA platform that can dynamically load haptic objects.

In the section, the prediction of forces and positions of the bodies in the mobile haptic interfaces are addressed when interacting with the virtual wall. We begin by comparing the force equations implemented to the forces that are recorded. Our discussion concludes with shortcomings of the work and areas of future work.

When the force equations are implemented, the simulation is in charge of the force exerted by the haptic device and sending the position of the end-effector to the second computer. A second computer is in charge of managing the control of the XY Table. The control of hardware devices are commonly done by a second computer in industry. The position of the XY table moves in the direction of the haptic device to keep the position of the haptic device arm within the force feedback workspace. This also positively improves the force output of the haptic device because in some cases the maximum output force requires some haptic arm

devices to have its robotic arm links in an orthogonal arm position as with the Sensable Phantom Omni.

We now have a better understanding of the forces of the end-effector from the haptic device and XY table when interacting with a virtual wall or haptic object while the XY table is moving the haptic device. It is seen that the force exerted by the haptic device is constant even though the XY table is moving. The communication time delay between the two computers has little effect on the force that is exerted. The largest error in the trials when the haptic device was not exerting the maximum force was 0.05 Newtons. This is small compared to the size of an adult hand used to input force to the end-effector of the haptic device. This work has shown that the error is small enough to have minimal to no effect experienced by the user.

There are certain limitations within this study that need to be addressed for future work in this field. The force output of the haptic device is small and limits the number of tasks that can be accomplished in virtual assembly processes. More work needs to be done to classify the system dynamics and to identify frictional forces and what is causing friction.

A more efficient method of measuring time of execution needs to be used for future uses. In the c++ programming language, the clock() function and constant CLOCKS_PER_SEC were implemented. Since CLOCKS_PER_SEC is the constant that is implementation defined of the system at 1000 H_Z, that does not mean the counter is actually implemented every millisecond. This may increase the possibility of having multiple values for this same time step.

Additionally, a natural extension of this study would be to investigate the application of mobile haptic interfaces and the forces exerted on the user with a large scale immersive environment such as a CAVE.

BIBLIOGRAPHY

[1] F. Gosselin, C. Andriot, F. Bergez and X. Merlhiot, "Widening 6-DOF haptic devices workspace with an additional degree of freedom," in *eurohaptics Conerence, 2007 and Symposium on Haptic Interaces for Virtual Environment and Teleoperator Systems*, 2007.

[2] G. Burdea, "Haptics issues in virtual environments," *Computer Graphics Internionał 2000 Proceedings,* pp. 295-302, 2000.

[3] P-J Fager, Per von Wowern, "The use of haptics in medical applications," *The Inernational Jouranl of Medical Robotics and Computer Assisted Surgery,* vol. 1, no. 1, pp. 36-42, 2004.

[4] W. Sherman and A. Craig, Understanding Virtual Reality, Boston: Morgan-Kaufmann Publishers, 2003.

[5] M. Heilig, "Sensorama Simulator". United States Patent 3050870, 28 August 1962.

[6] I. Sutherland, "The Ultimate Display," *Information Processing ,* vol. 2, pp. 506-508, 1965.

[7] T. Defanti and D. Sandin, "Final Report to the National Endowment of the Ars," University of Illinois at Chicago Circle, Chicago, IL., 1977.

[8] C. Cruz-Neira, J. Leigh, M. Papka, C. Barnes, S. Cohen, S. Das, R. Engelmann, R. Hudson, T. Roy, L. Siegel, C. Vasilakis, T. DeFanti and D. Sandin, "Scintists in wonderland: A report on visualizations applications in the CAVE virtual reality environment," *IEEE 1993 Symposium*

on Research Froniers, pp. 59-66, 25-26, 1993.

[9] F. Brooks, Jr., "What's real about virtual reality?," *Computer Graphics and Applications, IEEE,* vol. 19, no. 6, pp. 16-27, 1999.

[10] R. Mostrom, "Head Mounted Displays". United States Patent 3923370, 2 Decembe 1975.

[11] A. Craig, Developing Virtual Reality Applications, Burlington, MA, 2009.

[12] "Haptic - Definition and More from the Free Merriam-Webster Dictionary," Merriam-Webster Dictionary, 2012. [Online]. Available: http://www.merriam-webster.com/dictionary/haptic. [Accessed 5 March 2012].

[13] F. P. Brooks, Jr., M. Ouh-Young, J. J. Batter and P. Jeome Kilpatrick, "Project GROPE: Haptic displays for scientific visualization," *SIGGRAPH Compuer Graphics,* p. 24, 1990.

[14] H. Maekawa and J. Hollerbach, "Haptic display for object grasping and manipulating in virtual environment," *IEEE International Conference on Rootics and Automation,* vol. 3, pp. 2566-2573, 1998.

[15] M. Zinn, O. Khatib, B. Roth and J. Salisbury, "Large Workspace Haptic Devices - A New Actuation Approach," *Haptic interfaces for virtual environment and teleoperator systems,* pp. 185-192, 2008.

[16] G. Luecke and J. Beckman, "Haptic interactions with under-actuated robots using virtual mechanisms," *IEEE International Conference in Robotics and Automation,* pp. 2878-2883,

2008.

[17] J. Park and O. Khatib, "A haptic teleoperation approach based on contact force control," *International Journal of Robotics Research,* vol. 25, no. 5, pp. 575-591, 2006.

[18] K. Patel and S. Vij, "Locomotion inerface o the virtual environment to acquire spatial knowledge," in *TENCON 2008 - 2008 IEEE Region 10 Conference*, 2008.

[19] HAPTION, *Virtuose API V2.0 Progamming Manual,* 2004.

[20] E. Johnsen and W. Corliss, Human FActors Applications in Teleoperator Design and Operation, John Wiley & Sons, 1971.

[21] A. Fischer and J. Vance, "PHANToM haptic device implemented in a projection screen virtual environmnt," in *Proceedings of the workshop on Virtual environments*, New York, NY, 2003.

[22] F. Conti and O. Khatib, "Spanning Lage Workspaces using Small Haptic Devices," in *First Joint urohaptics Conference and Symposium on Haptic Interfaces for Virtual Environment and Teleopeator Systems*, 2005.

[23] L. Dominjon, A. Lécuyer, J. Burkhardt, G. Andrade-Barroso and S. Richir, "The "bubble" technique: interacting with alrge virtual environments using haptic devices with limited wokspace," in *Proceedings of World Hapics Conference*, Pisa, Italy, 2005.

[24] L. Dominjon, A. Lécuyer, J. Burkhardt and S. Richir, *A comparison of three techniqes to*

ineract in large virtual environments using haptic devices with limited workspace, 2006, pp. 288-299.

[25] M. Lin and M. Otaduy, Haptic Rendering: Foundations, Algorithms, and Applications, Wellesley, MA: A K Peters Ltd., 2008.

[26] H. Iwata, "Virtual Preambulator: A Novel Interface Device for Locomotion in virtual environments," in *IEE VRAIS* , 1996.

[27] H. Noma and T. Miyasato, "Design for locomoion inerface in a large scale virtual environment. ATLAS: ATR Locomotion interface for Active Self motion," in *ASME Dynamic Sstems and Control Division*, 1998.

[28] H. Iwata, "Walking about virtual envionments on an infinite floor," in *IEEE Virtual Reality* , Houston, TX, 1999.

[29] J. Hollerbach, R. Christensen, Y. Xu and S. Jacobsen, "Design Specification for the Second Generation Sacos Treadport Locomotion Interface," in *Haptics Symposium, Proceedings of ASME Dynamic Systems and Control Division*, Orlando, FL, 2000.

[30] H. Iwata, H. Yano, H. Fukushima and H. Noma, "CirculaFloor [locomoion interface]," *Computer Graphics and Applications,* vol. 25, no. 1, pp. 64-67, 2005.

[31] M. Hirose, K. Hirota, T. Ogi, H. Yano, N. Kakehi, M. Saito and M. Nakasige, "HapticGEAR: he development of a wearable force display system for immersive projection displays," in

Virtual Reality, Yokohama, Japan, 2001.

[32] E. Brau and F. Gosselin, "ICARE 3D: A New Liht 3D Hapic Interface," in *Eurohaptics*, Paris, France, 2006.

[33] A. Frisoli, F. Rocchi, S. Marcheschi, A. Dettori, F. Salsedo and M. Bergamasco, "A new force-feedback arm exoskeleton for haptic interaction in viual environments," in *Eurohaptics Conference, 2005*, 2005.

[34] Ishii and M. Sato, "A 3D Spatial Interface Device Using Tensed Strings," *Presence-Teleoperators and Virtual environments,* vol. 3, no. 1, pp. 81-86, 1994.

[35] M. Bouguila, M. Ishii and M. Sato, "A Large Workspace Haptic Device for Human-Scale Virtual Environments," in *First International Wokshop on Haptic Human Computer Interaction*, Glasgow, UK, 2000.

[36] F. Gosselin, C. Andriot, F. Bergez and X. Merlhiot, "Widening 6-DOF haptic devices with an additional degree of freedom," in *Eurohaptics Conference 2007 and Symposium on Haptic Interfaces for Virtual Environment and Teleoperator Systems*, 2007.

[37] L. Dominjon, J. Perret and A. Lécuyer, "Novel devices and interaction techniques for human-scale haptics," *The Visual Computer: International Journal of Computer Graphics,* vol. 23, no. 4, pp. 257-266, 2007.

[38] N. Nitzsche, U. Haneheck and G. Schmidt, "Design issues of mobile haptic interfaces,"

Journal of Robotic Systems, vol. 20, no. 9, pp. 549-556, 2003.

[39] R. A. Pavlik and J. M. Vance, "Expanding Haptic Workspace for Coupled-Object Manipulation," in *Proceedings of he ASME 2011 World Conference on Innovative Virtual Reality*, Milan, Italy, 2011.

[40] A. Seth, H. Su and J. Vance, "SHARP: A System for Haptic Assembly and Realistic Prototyping," in *Computers and Information in Engineering Conference, ASME*, 2006.

[41] A. Bierbaum, C. Just, P. Hartling, K. Meinert, A. Baker and C. Cruz-Neira, "VR Jugler: A Virtual Platform for Virtual Rality Application Development," in *Virtual Reality Conference, IEEE*, 2001.

[42] R. Pavlik and J. Vance, "VR JuggLua: A Framework for VR Applications Combining Lua, Open-SceneGraph, and VR Juggler," in *IEEE Virtual Reality*, 2011.

ACKNOWLEDGEMENTS

This thesis is dedicated to my brother and sister, Gilbert Garlington Jr. and Denise Sanchez, for always looking out for their “little brother.”

I would like to take this opportunity to express my gratitude to Dr. Vance for her guidance and support during the research process. She has been nothing short of supportive and patient with me and the hurdles encountered during the research process.

I would also like to thank Dr. Luecke for his patience and the many hours spent in his office and the lab discussing theories and directions to take the research. I have learned so much during my graduate studies under his advisement also. I would also like to thank Dr. Derrick Rollins for his efforts and contributions to this work as a committee member.

Ryan Pavlik, Patrick Carlson, and Leif Berg have all been invaluable in computer support. A special thanks to Chris Walck and Don Kieu for their assistance in developing the system setup.

I would like to thank my mother and my family for their support during my studies. Additionally, I would to like to thank my fraternity brothers in Sigma Lambda Beta for their help and emotional support while I am far away from home.

BIOGRAPHICAL SKETCH

Isaac Joel Garlington was born on May 8, 1988 in Kansas City, Kansas. He received the Bachelor of Science in Mechanical Engineering from Iowa State University in 2010 and the Master of Science in Mechanical Engineering in 2012. His thesis laid groundwork for understanding the force feedback in haptic interaction in a virtual environment using a mobile haptic interface. He has served as a Research Assistant in the Department of Mechanical Engineering at Iowa State University.